DEFENCE R&D DÉFENSE

The Canadian QWIP Experiment on the STRV Satellite

Shyam M. Khanna, Paul J. Thomas and H.C. Liu

Defence R&D Canada
TECHNICAL REPORT
DREO TR 2001-152
December 2001

National Defence Defense nationale

Canada

105-03245/

THE CANADIAN QWIP EXPERIMENT ON THE STRV SATELLITE

Shyam M. Khanna
Space Systems and Technology Section

Paul J. Thomas
Topaz Technology Inc.

H.C. Liu
National Research Council

Defence Research Establishment Ottawa

Technical Report

TR 2001-152

December 2001

© Her Majesty the Queen as represented by the Minister of National Defence, 2001

© Sa Majesté la reine, representée par le ministre de la Défense nationale, 2001

Abstract

This report describes the concept, design and implementation of the Canadian Quantum Well Infrared Photodetector (CA QWIP) experiment on the UK STRV 1D satellite. The objective of the experiment was to check the performance and verify the effect of nuclear radiation in the space environment on Quantum Well Infrared Photodetectors (QWIP), Quantum Well Light Emitting Diodes (QW LED) and QWIP/LED integrated devices designed and fabricated at the National Research Council (NRC) of Canada. The experiment was launched successfully on the STRV 1D satellite in November 2000. The CA QWIP experiment operated well in space soon after launch. Since then, the satellite itself has suffered a system failure that is not related to the CA QWIP experiment. This failure has prevented any communication from all experiments on the STRV 1C and 1D satellites from various countries including UK, Canada and US.

Résumé

Ce rapport décrit le concept, la conception et la mise en place de l'expérience concernant le *Quantum Well Photodetector* canadien *(CA QWIP)* sur le satellite *U-K STRV 1D*. L'objectif de l'expérience était de contrôler l'exécution et vérifier l'effet du rayonnement nucléaire dans l'environnement de l'espace sur les *Quantum Well Infrared Photodetectors (QWIP)*, les *Quantum Well Light Emitting Diode (QW LED)* ainsi que les détecteurs-émetteurs intégrés *QWIP/LED* conçus et fabriqués au Conseil National de Recherche Canada (CNRC). L'expérience a débutée avec succès sur le satellite de STRV 1D en novembre 2000. L'expérience *CA QWIP* a bien fonctionné dans l'espace peu après la satellisation. Depuis ce temps, le satellite lui-même a souffert une panne de système qui n'est pas reliée à l'expérience CA QWIP. Cette panne a empêché toute transmission de toutes les données concernant les expériences sur les satellites *STRV 1C* et *1D* de divers pays incluant le R-U, le Canada et les É-U.

This page intentionally left blank.

Executive summary

Defence Research and Development Canada (DRDC) has a Space R&D Program that supports the space-policy objectives of the Canadian Department of National Defence (DND). In support of the Program, DRDC worked out an arrangement with the UK Defence Evaluation & Research Agency (DERA) and the US Ballistic Missile Defense Organization (BMDO) to participate in an experimental micro-satellite program called the UK Space Technology Research Vehicle (STRV). The US Air Force integrated the CA and several other US experiments on the US Experimental Test Bed (ETB). The ETB in turn was integrated to the STRV 1D satellite by DERA.

The quantum well technology provides a highly flexible approach for the development of quantum well infrared photodetectors (QWIP) and light emitting diodes (QW LED). These devices provide a promising new class of infrared detectors and emitters whose wavelength of operation can be adjusted over a wide infrared wavelength region. Further, ground-based nuclear radiation studies indicated that QWIPs and QW LEDs are more radiation damage tolerant than conventional infrared (IR) detectors and emitters respectively. In addition, NRC of Canada has developed a novel QWIP/LED integrated IR photodetector which has several advantages over a conventional QWIP.

This report describes briefly the concept, design, fabrication, test and launch in space of the Canadian Quantum Well Infrared Photodetctor (CA QWIP) experiment. This includes the development of QWIPs, QW LEDs, and QWIP/LED devices; a passive cryocooler for cooling these devices to low temperatures; a special electronics board for device characteristics measurements in space; and the integration of the CA QWIP experiment on US BMDO Experimental Test Bed (ETB).

The UK STRV 1D micro-satellite was designed to fast-track the latest space technology into orbit. The satellite carried a variety of hardware and software experiments from several countries including the US, Canada and UK into the harsh space environment of the geosynchronous transfer orbit (GTO). In this orbit, the satellite passes through all of the major zones of natural radiation and thus allows comprehensive testing of new technologies, components and detectors.

The STRV 1D was launched on November 14, 2000 on an Ariane-5 launch vehicle, carrying the Canadian QWIP experiment. The QWIP experiment operated successfully from space soon after launch. Since then, the STRV 1C and 1D spacecrafts has suffered a system failure shortly after launch that has broken the communications link to the ground from all space experiments. No further data from the CA QWIP has been received since that time.

Khanna, S.M., Thomas, P.J. 2001, Liu, H.C., THE CANADIAN QWIP EXPERIMENT ON THE STRV SATELLITE. DREO TR 2001-152. DEFENCE RESEARCH ESTABLISHMENT OTTAWA.

Sommaire

Recherche et développement pour la défense Canada (RDDC) a un programme de R&D pour l'espace qui supporte les objectifs du département de la défense nationale (DDN). À l'appui du programme, RDDC a établi un accord avec *the UK Defence Evaluation & Research Agency (DERA)* et *the US Ballistic Missile Defense Organization (BMDO)* afin de participer à un programme expérimental de micro-satellite appelé *the UK Space Technology Research Vehicle* (STRV). Les forces aériennes des É-U ont intégré l'expérience canadienne et plusieurs autres expériences des É-U sur le *US Experimental Test Bed (ETB)*. Le *ETB*, à son tour, a été intégré au satellite de *STRV 1D* par *DERA*.

La technologie *quantum well* fournit une approche fortement souple pour le développement du détecteur photoélectrique infrarouge *quantum well (QWIP)* et pour la diode électroluminescente *(QW LED)*. Ces appareils fournissent une nouvelle classe de détecteurs et d'émetteurs infrarouges dont la longueur d'onde d'opération peut être ajustée au-dessus d'une région large de longueur d'onde infrarouge. De plus, les études qui ont été accomplis à terre ferme indiquent que les *QWIPs* et les *QW LEDs* peuvent tolérer plus de dommage dû au rayonnement nucléaire que les détecteurs et émetteurs infrarouges (IR) conventionnels respectivement. En outre, le CNRC a développé un détecteur et émetteur photoélectrique IR intégré (*QWIP/LED)* qui a plusieurs avantages par rapport à un *QWIP* conventionnel.

Ce rapport décrit brièvement le concept, la conception, la fabrication, l'essai et la satellisation de l'expérience infrarouge de photo détecteurs *quantum well* canadien *(CA QWIP)*. Ceci inclut le développement des appareils *QWIPs*, *QW DEL*, et *QWIP/LEDs*; un cryoréfrigérateur passif pour refroidir les appareils à de basses températures; une carte électronique pour effectuer des mesures de caractérisation dans l'espace, et l'intégration de l'expérience CA QWIP sur le *US BMDO Experimental Test Bed (ETB)*.

Le micro-satellite *UK STRV 1D* était conçue pour promouvoir rapidement technologie de l'espace la plus récente en orbite. Le satellite a porté une variété de matériaux et d'expériences de logiciel de plusieurs pays comprenant les É-U, le Canada et le R-U dans l'environnement sévère du *geosynchronous transfer orbit (GTO)*. Dans cette orbite, le satellite traverse toutes les zones principales du rayonnement naturel et permet ainsi le test complet de nouvelles technologies, de composants et de détecteurs.

Le *STRV 1D* a été satellisé le 14 novembre, 2000 sur un véhicule de lancement Ariane-5, portant l'expérience canadienne *QWIP*. L'expérience *QWIP* a fonctionné avec succès peu après la satellisation. Depuis ce temps, les vaisseaux spatiaux *STRV 1C* et *1D* ont souffert une panne de système qui a rompu le lien de communication des expériences dans l'espace avec la terre ferme. Aucune donnée supplémentaire du *CA QWIP* n'a été reçue depuis cet évènement.

Khanna, S.M., Thomas, P.J. 2001, Liu, H.C., L'ÉXPÉRIENCE CANADIENNE QWIP ABORD DU SATELLITE *STRV*. DREO TR 2001-152. CENTRE DE RECHERCHES POUR LA DÉFENSE OTTAWA.

Table of contents

Abstract i

Executive summary iii

Sommaire iv

Table of contents iv

List of figures vii

List of tables ix

1. Introduction 1
   1.1 The QWIP Experiment Concept 2

2. Quantum Well Devices and Ground-Based Measurements 4
   2.1 Radiation Effects on Quantum Well Infrared (IR) Devices 6

3. Payload Concept and Circuit Requirements 10
   3.1 Payload Concept 10
   3.2 Electronics Control Board Design 11
   3.3 Implementation of the Electronics Board 16

4. Passive Cryocooler 19

5. Interface of the CA QWIP Experiment with the STRV 1 D Spacecraft 28
   5.1 Mechanical Interface 28
   5.2 Electrical and Signal Interfaces 30

6. Data Processing 31

7. Tests 35
   7.1 Electronics Tests 35
      7.1.1 Electrical Power Consumption 36
   7.2 Cryocooler Tests 36
   7.3 Space-Based Tests 38

8. Conclusions 39

9. References 41

List of figures

Figure 1. STRV Spacecraft and its Orbit 1

Figure 2. Time Scales in the QWIP Experiment 3

Figure 3. Layered structure of quantum well device 4

Figure 4. Novel QWIP readout approach 5

Figure 5. Energy-band sketch of integrated QWIP-LED. 5

Figure 6. Dark current vs. voltage characteristics at 77 K of a QWIP irradiated with 3 MeV protons at various fluence levels. 7

Figure 7. Spectral responsivity versus wavelength characteristics for a QWIP irradiated with protons at different fluence levels. 7

Figure 8. Device operability vs. fluence for a QWIP for irradiation with different particles. 8

Figure 9. Normalized light intensity of a QW LED on irradiation with protons at different energies 9

Figure 10. Bridge Circuit 12

Figure 11. Schematic of control circuit concept 13

Figure 12. Timing and Address circuit concept 15

Figure 13. Implementation of electronic switching 17

Figure 14. Photograph of flight electronic board 18

Figure 15. Passive cryocooler concept 20

Figure 16. Placement of devices under test on cold plate 21

Figure 17. Schematic of radiative exchange between the payload and surroundings 22

Figure 18. Top view of assembled system showing passive cryocooler 23

Figure 19. Insulating struts on cryocooler 24

Figure 20.Side view of the cryocooler during assembly 25

Figure 21. Wiring of the devices under test 26

Figure 22. Rejection of sunlight by the cryocooler 27

Figure 23.Schematic of electrical and mechanical connection in the CA QWIP Experiment . 28

Figure 24.Schematic of connection of the QWIP Experiment to the MFS 29

Figure 25. Analysis data flow diagram..... 32

Figure 26. End temperature of cryocooler components..... 37

Figure 27. Cryocooler end temperature with load..... 37

List of tables

Table 1. Evaluation Methodology 10

Table 2. Key parameters of the I-V measurements. 11

Table 3. Electronics highlights. 14

Table 4. Cryocooler requirements. 19

Table 5. Passive cryocooler features. 21

Table 6. Data processing highlights. 33

Table 7. Summary of electronics tests. 35

Table 8. Power for different board modes. 36

Table 9. Status summary. 39

1. Introduction

Defence Research and Development Canada (DRDC) has a Space R&D Program that supports space-policy objectives of the Canadian Department of National Defence (DND). This is achieved through the development of capabilities in space systems, sub-systems and technologies; space environment and advanced electronics; space-based radar; infrared and visible wavelength space surveillance systems; surveillance of space; and warning and defence systems.

In support of this Program, DRDC worked out an arrangement with both the UK Defence Evaluation & Research Agency (DERA) and the US Ballistic Missile Defense Organization (BMDO) to participate in a twin micro-satellite experimental program called UK Space Technology Research Vehicle (STRV) 1C and 1D [1]. These two microsats were designed to fast-track the latest space technology to orbit. The satellites carried a variety of hardware and software experiments into the harsh space environment of the geo-synchronous transfer orbit (GTO). In this orbit, the satellites pass through all of the major zones of natural radiation [2]. This allows for comprehensive testing of new technologies, components and detectors. Figure 1 shows the STRV orbit and the orientation of the Canadian Quantum Well Infrared Photodetector (CA QWIP) experiment. Because the QWIP experiment is facing in a direction normal to the equatorial plane, it sees 'cold space' most of the time. Hence passive cryocooling is an option for achieving the low temperature required for QWIP operation.

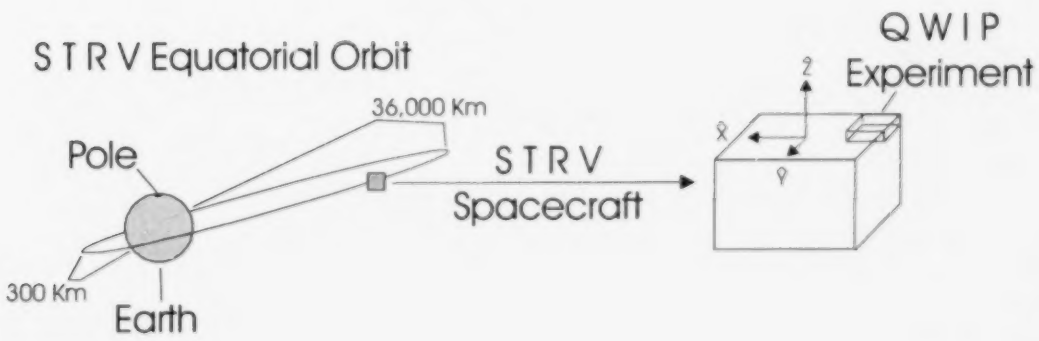

Figure 1. STRV Spacecraft and its Orbit

The 14 November 2000 launch of STRV-1C and 1D was the first "piggy-back" launch on an Ariane-5 launcher, with the micro-satellites accommodated beneath the main satellite within the nose cone. Ariane-5 offers reasonably large usable mass and volume for piggyback flight

at relatively low cost. DRDC had three experiments on these two UK STRV satellites. The rest of the experiments were sponsored by a wide variety of space organizations in the UK, continental Europe, and the US (NASA, US AFRL and BMDO). The data from the experiments sponsored by BMDO and DRDC was to be shared by the two organizations for their internal use under a data sharing arrangement.

This document describes the CA QWIP experiment, which was one of the three Canadian experiments on these satellites. The experiment resulted from collaboration between two establishments of DRDC- the Defence Research Establishment Ottawa (DREO) and Defence Research Establishment Valcartier (DREV), the Institute of Microstructural Sciences (IMS), National Research Council (NRC) of Canada and the Centre for Research in Earth and Space Technology (CRESTECH), based in Toronto, Canada. The CA QWIP experiment includes a set of quantum well infrared photodetectors (QWIPs), quantum well light emitting diodes (QW LEDs) and QWIP/LED detector/emitter integrated devices that have been developed for infrared imaging [3], [4], [5], [6]. These detectors are being tested for space applications. The detectors were mounted on a passive cryo-cooler, also developed in Canada [7], for cooling the detectors to low temperatures in the space environment. The US BMDO integrated the CA QWIP experiment on the Experimental Test Bed (ETB) at the US Air Force Research Laboratory (US AFRL), Albuquerque, NM. The ETB had a number of other experiments from different US organizations. The ETB provided the control, power, digitization, memory and communication functions to all of these experiments including the CA QWIP experiment.

The newly developed quantum well technology provides an elegant and extremely flexible method for fabricating mid to far-infrared (IR) photo detectors. In particular, the technology is suited to the fabrication of large 2D detector arrays at any wavelength in the 3 to 20 μm spectral region. Further, it is particularly suitable in terms of weight, size and cost for space applications.

1.1 The QWIP Experiment Concept

The electronics for the QWIP experiment is basically a bridge circuit. Each of the four resistive arms of the bridge has a value that is selected by a bank of electronic switches. The switch states, in turn, are set by the output of a PROM. At power-on, the PROM address is set to address 0 (out of 569 possible values). Whenever a suitable trigger pulse waveform is received by the electronics, the PROM address is incremented and the switch states may change. Nominally, the ETB on the spacecraft sends such a trigger waveform once per minute. After a brief delay to allow the analog signal to achieve equilibrium, the ETB reads the analog output of the QWIP experiment. The ETB then digitizes the analog outputs (two outputs, into a pair of bytes), stores the data and arranges for downloading to the ground every 2 to 3 days.

There is no timing information stored with the digital data. Under normal operating conditions, the PROM address will be incremented once per minute. The time of power-on to the QWIP experiment is known to the ETB and is expected to be available to the ground processing software. Hence, the time of each trigger waveform to the QWIP experiment from

the ETB can be calculated. Furthermore, a relative time stamp can be calculated for each measurement by consideration of the position of the data point in the measurement sequence, the temperature at that point and other factors that can be inferred from the data sequence.

The various time scales in the QWIP experiment are indicated in Fig. 2. For a nominal mission duration of 52 weeks, data is downloaded from the STRV about once a week when the satellite orbit brings it close to the download station in England. The data is then placed on a web site. Each data sequence lasts from 10^0 to 10^3 minutes, with a measurement approximately every minute. A data sequence is terminated by shutdown of power to the experiment.

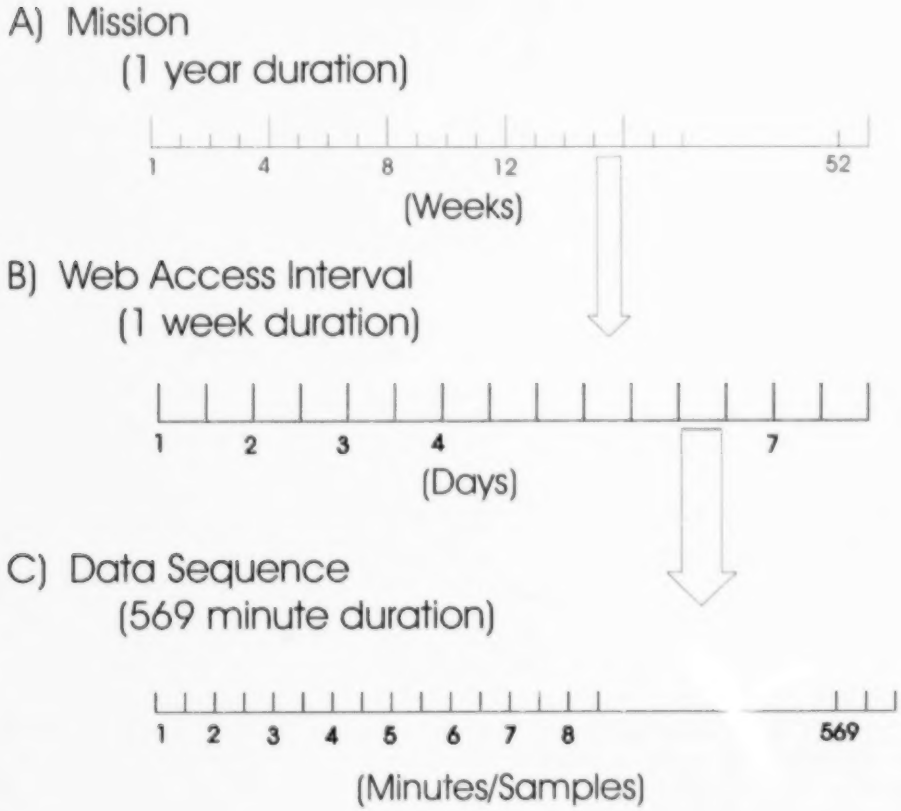

Figure 2. Time Scales in the QWIP Experiment

The data sequences are analyzed by calculating a 'device under test resistance' for each measurement. By comparing the values with models, the time and other information, the resistance of the device under test can be corrected for temperature, supply voltage and other systematic errors. This experiment will provide an estimate of the fractional change in resistance of each of the three types of devices (QWIP, LED and QWIP/LED) as a function of nuclear radiation fluence at the time of measurement.

2. Quantum Well Devices and Ground-Based Measurements

A conventional QWIP device is a layered structure, as indicated in Fig. 3. In general, such devices are bulk bonded to a silicon chip for device readout measurement.

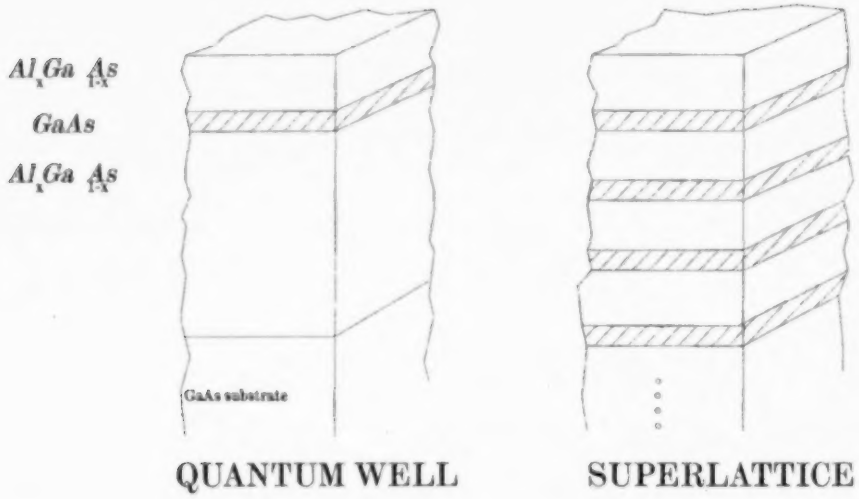

Figure 3. Layered structure of quantum well device

Recently, Liu et al. [3] have demonstrated an integrated device consisting of a QWIP and a light emitting diode (LED) by epitaxially growing a quantum well light emitting diode (QW LED) directly on top of the QWIP. This unique approach avoids hybrid bonding and thermal mismatch between the GaAs QWIP and the hybrid bonded Si chip used in the conventional system. Figure 4 shows the differences between conventional QWIP device readouts and the new concept. The integrated QWIP/LED device acts as a converter of the incident mid to far-IR radiation that is detected by the QWIP to near-IR radiation that is emitted by the LED. A conventional charge coupled device (CCD) chip can measure the radiation emitted by the LED. This technique could lead to a simpler and cheaper method for the production of a QWIP IR camera. Further, a QWIP/LED detector array could lead to pixel-less infrared imaging that would represent substantial simplification of the detector array processing [4], [5]. Further, the peak response of the multicolour QWIP detector can be changed by adjusting the applied voltage across a stack of different colour QWIPs. This provides the possibility of developing a multi-spectral imaging sensor using a given QWIP device by externally adjusting the applied voltage across the device [6].

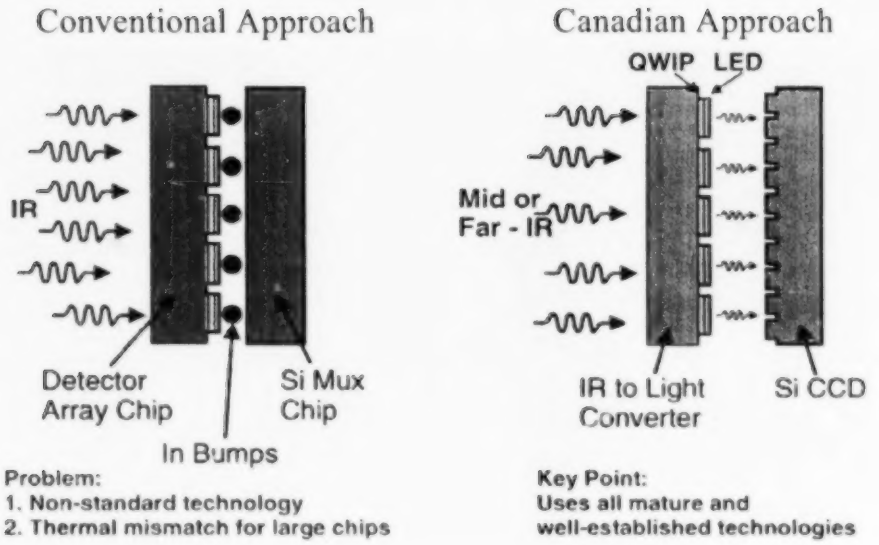

Figure 4. Novel QWIP readout approach

An energy-band description of a QWIP/LED structure is shown in Fig. 5.

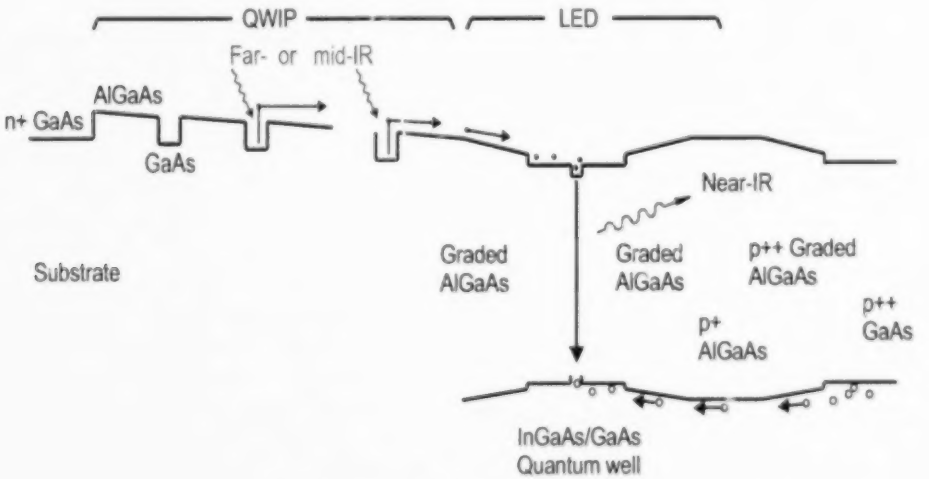

Figure 5. Energy-band sketch of integrated QWIP-LED.

A bias voltage is applied across the entire QWIP/LED structure. When a thermal photon creates an electron, the electron is transported with high efficiency to the LED structure where it has a high probability of generating a near-infrared photon. The collection of the near-

infrared photons by suitable optics for readout by a silicon imager is the final step in the Canadian approach as was indicated in Fig. 4-5.

2.1 Radiation Effects on Quantum Well Infrared (IR) Devices

In space, nuclear radiation can cause displacement damage to the semiconductor lattice of the solid state device and degrade/ destroy the device performance progressively with time. Through extensive radiation studies on ground, Khanna et al. have shown that QWIPs are quite radiation hard [8]. However, the GaAs LEDs are well known to be quite sensitive to nuclear radiation. Recently, Khanna et al have also shown that GaAs QW LEDs are more radiation hard than the conventional GaAs LEDs [9], [10]. High-energy protons can cause most of the permanent damage in the space environment, since they occur at relatively high fluence and are shielded only partially by the spacecraft skin. Displacement damage by protons is an important limiting factor to the use of conventional GaAs light emitting diodes and related devices in space.

Two types of QWIPs, one operating at 3.7 μm and the other at 10.7 μm, were fabricated and tested on the ground. The 3.7 μm QWIP, along with LEDs and QWIP/LEDs, were used for the space experiment. The QWIP/LED device wafer is grown by molecular beam epitaxy on a 3 inch. semi-insulating GaAs substrate. The QWIP active region consists of 32 repeats of a double barrier quantum well with 4.5 nm GaAs wells, 2 nm AlAs confining barriers, and 30 nm barriers of Al(0.45)Ga(0.55)As. The wells are center delta-doped with Si to $3\times10^{11}/cm^2$. The LED active region is a 7 nm In(0.2)Ga(0.8)As well confined by 30 nm GaAs and graded AlGaAs, similar to the active region of a state-of-the-art Quantum Well laser. The mesa devices are made by standard GaAs micro-fabrication techniques with alloyed NiGeAu n-type and TiPtAu p-type contacts. Three devices sizes are made: 290 μm x140 μm, 460 μm x260 μm, and 900 μm x500 μm and are identified as small, medium and large respectively. Ring contacts are fabricated on top of the mesas for LED emission with optical windows of 200 μm x100 μm, 400 μm x200 μm, and 800 μm x400 μm for the three device sizes, respectively.

Laboratory measurements for nuclear radiation effects on QWIP, LED, and QWIP/LED devices have been conducted with protons and alpha radiations by Khanna et al.[8], [9]. The particle energy ranged from 1-500 MeV for protons and 1-15 MeV for alpha particles. The fluence ranged from 10^9 to 10^{16} cm^{-2}. We include a few results from these measurements for completeness and discussions. For QWIPs, dark current - voltage characteristics and spectral response were measured at low temperatures as a function of high energy nuclear radiation fluence. Figures 6-7 give dark current characteristics and spectral response respectively of a QWIP as a function of 3 MeV proton fluence.

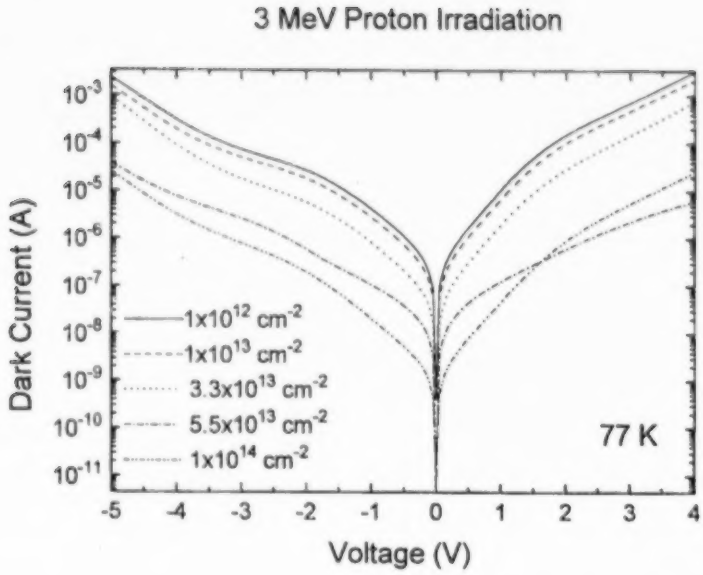

Figure 6. Dark current vs. voltage characteristics at 77 K of a QWIP irradiated with 3 MeV protons at various fluence levels.

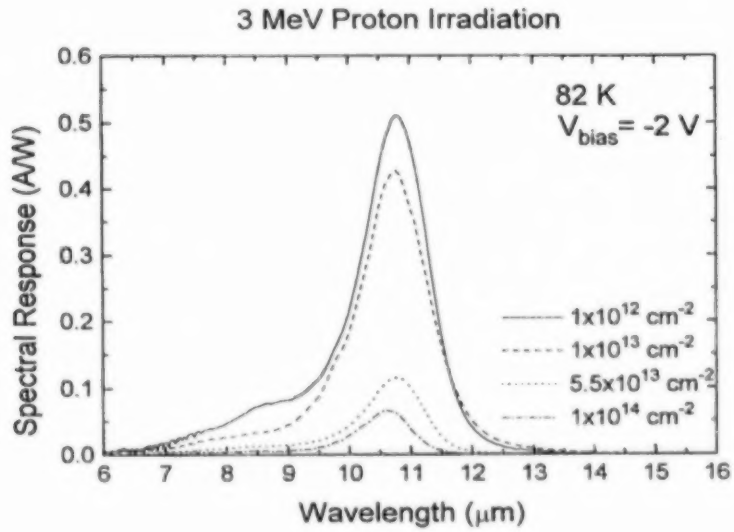

Figure 7. Spectral responsivity versus wavelength characteristics for a QWIP irradiated with protons at different fluence levels.

These results show that the dark current in the QWIP devices decreases dramatically with fluence. The current decreased progressively with increased fluence up to $1x10^{14}$ p/cm^2. On the other hand, the responsivity of the QWIP decreased but at a much slower rate with increased fluence as shown in Fig. 7. There is no change in the wavelength for peak response of these devices on irradiation.

In order to compare damage due to different particles at various energies, we compare device operability, which is defined as the responsivity of the irradiated QWIP normalized to its responsivity before irradiation. Figure 8 gives the device operability of a QWIP vs. fluence for irradiation with protons and alpha particles at different energies. This figure shows clearly that QWIPs are relatively quite radiation hard and would make ideal IR imaging sensors for space applications.

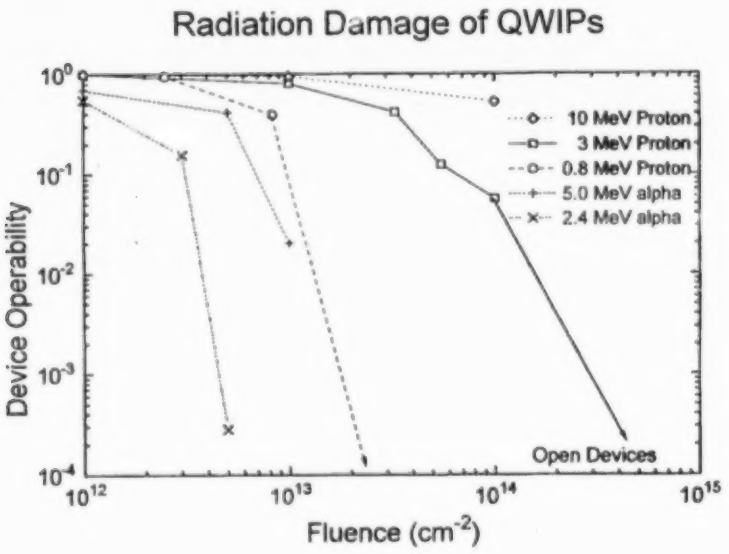

Figure 8. Device operability vs. fluence for a QWIP for irradiation with different particles.

Figure 9 shows the normalized light emission from a QW LED used in these experiments. LEDs are known to be quite susceptible to nuclear radiations. Khanna et al. [9] have shown that these QW LEDs are more radiation hard than any GaAs LEDs devices reported recently [10]. These QW LEDs are also harder than GaAs LEDs produced through the standard diffusion process or the double-heterojunction GaAs LEDs. Fig. 9 shows that the light emission from the LEDs is markedly reduced at $1x10^{13}$ p/cm^2 10 MeV proton fluence. Thus, these LEDs are more susceptible to radiation damage than the QWIP devices. The current-voltage characteristics of these LEDs were not much affected on irradiation [9]. These results

on QWIPs and QW LEDs show clearly that these devices are ideally suited for IR imaging from space.

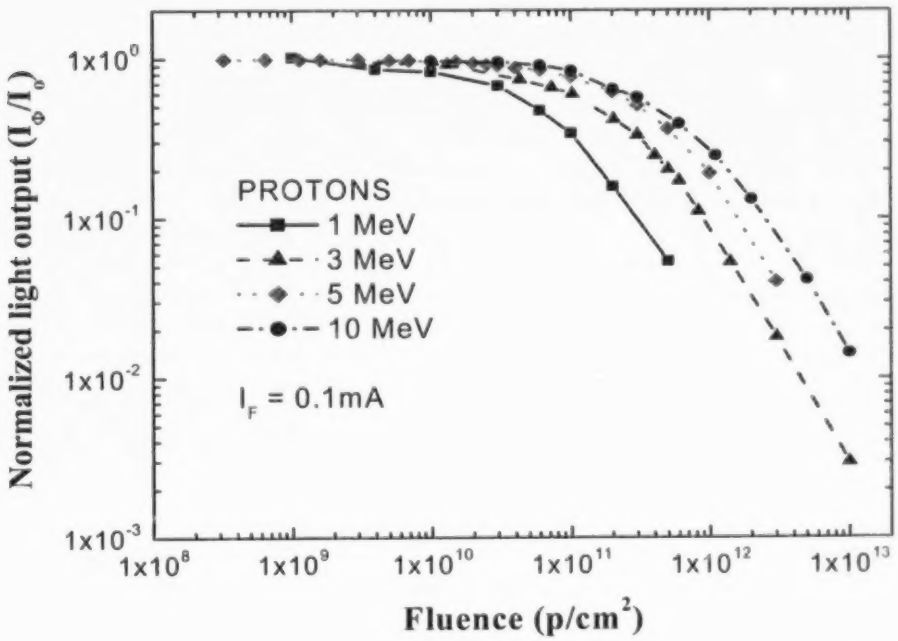

Figure 9. Normalized light intensity of a QW LED on irradiation with protons at different energies

3. Payload Concept and Circuit Requirements

3.1 Payload Concept

The highlights of the QWIP evaluation methodology are summarized in Table 1. The dark current characteristics of the devices are measured rather than optical performance, for convenience in the measurement process. Use of a geostationary transfer orbit (GTO) allows the annual proton and electron fluences to be an order of magnitude higher than the expected fluences in low earth orbit. Hence, a modest mission lifetime and a micro-satellite can be expected to achieve the measurement goals. The devices to be tested were selected for operation at about 150 K, a temperature that can be reached with a passive cryocooling method. While QWIP devices for infrared detection generally operate below 77 K, in order to reduce noise, the similarities in device response to radiation damage allow the use of QWIP devices with wider effective bandgap for the radiation damage studies. These devices operate at the higher temperature cited above. The Canadian QWIP experiment is a sub-experiment of the Electronic Test Bed (ETB) of the US BMDO and takes advantage of the control, power, digitizer, memory and communications functions of the ETB.

Table 1. *Evaluation Methodology*

Step	Description
Current/voltage curves	It is easier to measure dark current characteristics of these devices accurately than their optical performance.
Enhanced space radiation environment	The geostationary transfer orbit of the STRV satellite provides an annual fluence that is about 10 x the expected fluence in low-earth orbit.
Representative devices	Suitable QWIP IR detectors and LEDs were developed that could provide radiation sensitivity data for these devices at ~150K that can be attained by a small size passive cryocooler.
Uncontrolled environment	The temperature was allowed to drift with orbital position, and was sensed rather than controlled.
Paired devices	The devices under test are grouped in identical pairs, separated by a known amount of metal shielding. This technique allows a differential measurement of radiation effects under investigations.
Part of ETB	The Canadian QWIP experiment is a sub-experiment of the Electronic Test Bed (ETB) of the US BMDO and takes advantage of the control, power, digitizer, memory and communications functions of the ETB.

The temperature of the experiment was allowed to drift, and the temperature was measured on an ongoing basis. This mode of operation was preferred over active temperature control, in order to reduce power consumption, enhance reliability and reduce experiment mass. Suitable data processing methods were developed to compensate for temperature variations due to the

appearance of the earth in the field of view of the cryocooler when the satellite is close to the earth. The devices under test were 'paired' in order to minimize temperature and other systematic errors.

3.2 Electronics Control Board Design

The design concept of the 'state machine electronics control board' is simple, resistant to many single-point failure modes and readily ported to a chip-level implementation for situations where micro-power operation, very high radiation tolerance and low cost are important considerations.

Radiation effects on the photoresponse and noise of a QWIP infrared detector are the parameters of interest in this implementation of the circuit concept. The current-voltage (I-V) characteristics of a QWIP device is convenient to measure and can be used to predict its behaviour as a photodetector under the same conditions [4,5]. The I-V curve measurement approach is used in this work. Thus, the basic measurement is the resistance of QW devices under known or calculated voltage and temperature conditions. Selected parameters of the measurement scenario are identified in Table 2.

Table 2. *Key parameters of the I-V measurements.*

#	property	units	Target value	Notes
1	Sensitivity	%	0.1	To a change in resistance at a fixed voltage
2	Minimum current	A	10^{-6}	Includes both systematic and random errors
3	Maximum current	A	10^{-3}	Upper limit is set by expected self-heating
4	T_{min}	K	253	Lower limit of operating temperature range
5	T_{max}	K	313	Upper limit of operating temperature range
6	Response time	sec	1	Longer than settling time of analog circuit
7	Radiation tolerance	kRad	100	2 years in 10 hour geo-transfer orbit.
8	Temperature coefficient of devices	K^{-1}	.05	This parameter is the fractional change in QWIP device resistance per degree of temperature change.

The sensitivity is determined by the expected variation of the I-V curve with radiation. Ground-based measurements indicate a low sensitivity to radiation damage. Changes at the 0.1% level are comparable to the expected pixel spatial non-uniformity of a QWIP detector array and so were considered appropriate as a resolution limit.

QWIP devices can often be modeled as diodes and can have a strong exponential dependence of forward current on voltage. The minimum current is set by the largest equivalent resistance to be measured and the measurement voltage, and is influenced by noise considerations. The effects of radiation may be more apparent at low current [6]. Self-heating and need for low power consumption limit the maximum current.

The electronics board is mounted on the spacecraft and is tightly coupled thermally to the spacecraft structure, so that temperature range of operation of the electronic board is dictated by the spacecraft nominal internal operating temperature range. The total dose per year is expected to be about 50 kRad/year for the STRV 1D orbit, which is a geo-transfer orbit with a transit of the Van Allen belts twice per 10-hour orbit [3,6].

The operating concept is to acquire data every few minutes from each of the quantum well devices, temperature sensors and reference resistor. The data is transferred to the STRV computer system and stored for batch-mode transmission to a ground station. Data is desired over months or longer. Approximate time information is desirable in order to correlate anomalies in the data with solar flares or other transient ionizing radiation events. Temperature and bridge voltage measurements may be needed periodically in order to correct for systematic errors. The baseline measurement method is the use of a Wheatstone bridge circuit (Fig. 10). Thin-film metal resistors are used as the bridge elements due to their insensitivity to radiation damage.

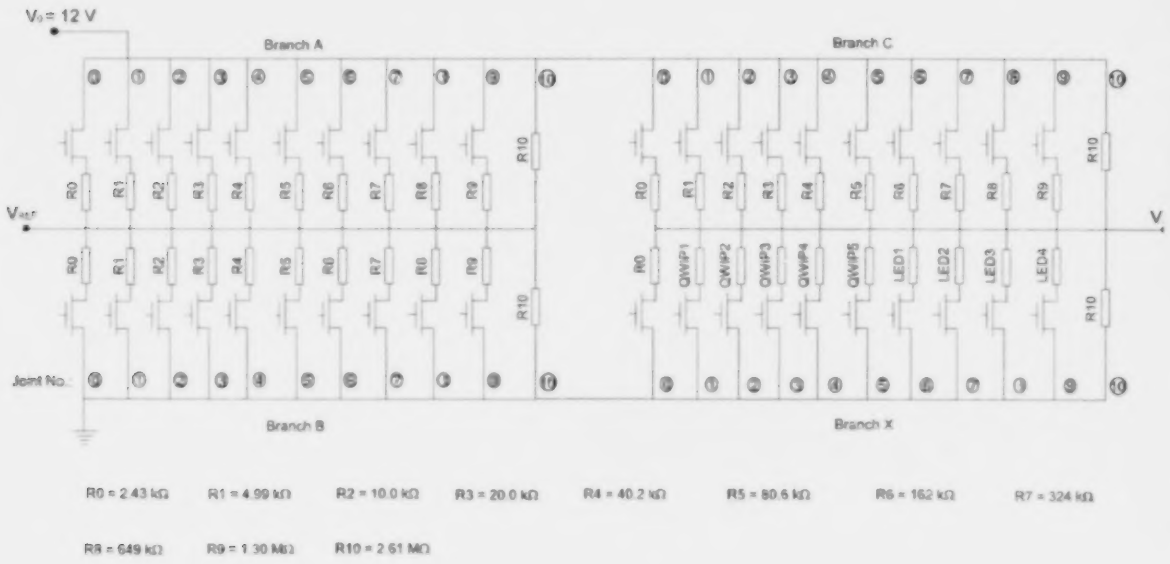

Figure 10. Bridge Circuit

By incorporating electronic analog switches into the bridge, the bridge resistances can be varied to match the resistance of the 'device under test' (DUT) and change the voltage across the device. The bridge mismatch voltage is amplified and provided to an external signal port for digitization and storage by the STRV spacecraft and its subsystems. Power to the bridge and the control circuitry is provided by the spacecraft. The bridge voltage is monitored by a calibration resistor that can replace the device under test in the bridge. The number of analog switches and resistors in each arm of the bridge can be tailored to the application. In this application, 16 switches were used in the 'device under test' arm of the bridge (to allow four each of three different types of QW devices, three temperature sensors and a calibration

resistor). Although shown schematically as transistors, each switch is a part of a space-qualified integrated circuit analog switch device. The bridge resistor values were carefully selected to provide the desired current and voltage measurement points at the expected operating temperature in space. The temperature coefficient of QWIP resistance is a dominant parameter in the design of the measurement system. Small temperature changes cause shifts in resistance that are large compared to the effects of radiation damage. The circuit design and the analysis procedures have been tailored to compensate for temperature effects.

The control circuit concept is shown in Figure 11. Starting from a reference state that is set during power-on, the state of the circuit is incremented by the RS422 input from the STRV satellite and its subsystems. The "*core electronics*" has a "*state memory*" that sets the outputs of the "*device control*" block, which in turn connects to analog and digital lines of the "*device under test*". Output digital values of the "*state memory*" are set by the "*timing and address circuit*".

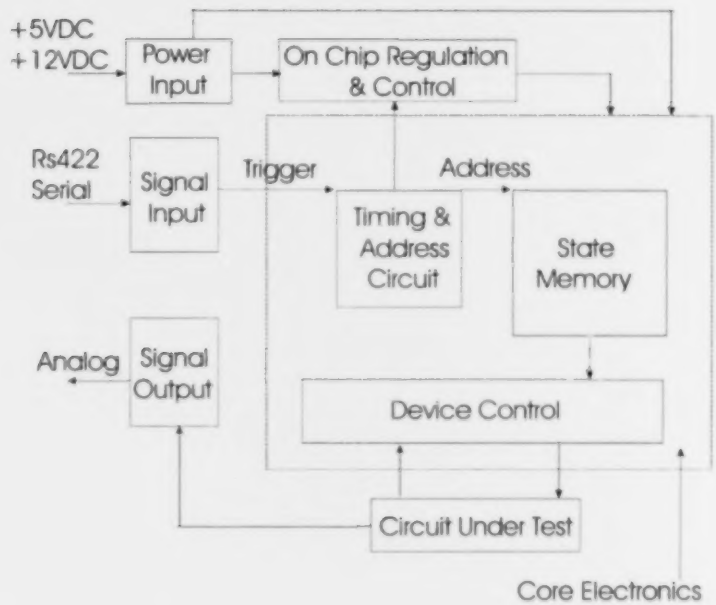

Figure 11. Schematic of control circuit concept

In response to a pulse train on the RS422 input lines, a "*trigger*" is asynchronously generated by the "*signal input*" block. This trigger increments the "*state memory*". After a suitable time delay, the "*signal output*" block settles to one or more analog (or digital) output levels that are available to an external circuit. Power to different circuit blocks ("*on-chip regulation and control*") is also linked to the "*timing and address circuit*".

A version of the circuit concept has been implemented with discrete components to measure the radiation dependence of the I-V curves of QW devices on the STRV 1 D spacecraft

following the requirements enunciated in Section 2. Note that the "*core electronics*" block of Figure 11 can be readily ported to a single CMOS chip.

In the present (discrete) circuit, the "*state memory*" is a PROM, the "*device control*" is a set of 32 discrete analog switches and the "*signal output*" is an operational amplifier that amplifies and buffers the bridge mismatch voltage from the "*circuit under test*". The "*timing and address circuit*" is fundamentally a counter that increments each time a pulse train on the RS422 lines causes a trigger to be generated by the "*signal input*".

Highlights of the design are described in Table 3.

Table 3. *Electronics highlights.*

Item	Notes
Wheatstone bridge	Sensitivity is independent of current or voltage to first order.
Electronic switches to change bridge resistances	All QW devices, the temperature sensors and the calibration resistor use the same bridge components.
Dual-channel amplifier	Two amplifiers in parallel with different gains allow higher sensitivity while preserving dynamic range.
Triggered 'state-machine' control	Each control sequence from the ETB increments the PROM that determines the states of the electronic switches.
Power control	Power-hungry components are turned off when not needed.

Use of a Wheatstone bridge allowed the sensitivity to be higher than the resolution of the ADC provided by the ETB, and also to be independent of the current or voltage level (to first order). The accuracy of a resistance measure is then dependent on the stability of the values of the bridge resistances. The bridge resistors are metal film resistors with temperature coefficient of about 50 ppm/K and negligible change with radiation. The effective bridge resistance includes the resistance of the electronic switch which was nominally about 50 ohms and did show both temperature and radiation sensitivity. The bridge resistance variations could be estimated during the analysis of the data sets, and were small enough (typically less than 0.1 %) to be a second-order effect.

A dual-channel amplifier was used. Each amplifier generally had a different gain. The high-gain channel provided better precision in bridge-mismatch voltage measurement but was sensitive to the temperature in that a temperature much different from the expected value would cause the voltage to be out of range. When the high-gain value was out of range, the low-gain value could still be used to provide a measurement with a reduced level of precision (typically a 2x reduction, from 0.1% to 0.2%).

The 'triggered state-machine' organization of the circuit was very robust. The states were stored in a rad-hard PROM. Most single-point failures would cause only minimal disruption

to the overall data reliability and usefulness. The triggering of the operation from the ETB allowed the average power dissipation to be reduced by 4x, leading to the operation of the QWIP experiment at all times in the mission. By contrast, other experiments would be powered down occasionally to avoid excessive STRV system power drain.

The timing and address circuit is shown in more detail in Fig. 12. The input to the "*timing and address circuit*" is a trigger signal generated by a pulse train on the RS422 lines. Currently, the *"signal input"* is generated by a capacitor and monostable and is intended to filter out possible fast transients from other activity on the RS422 lines.

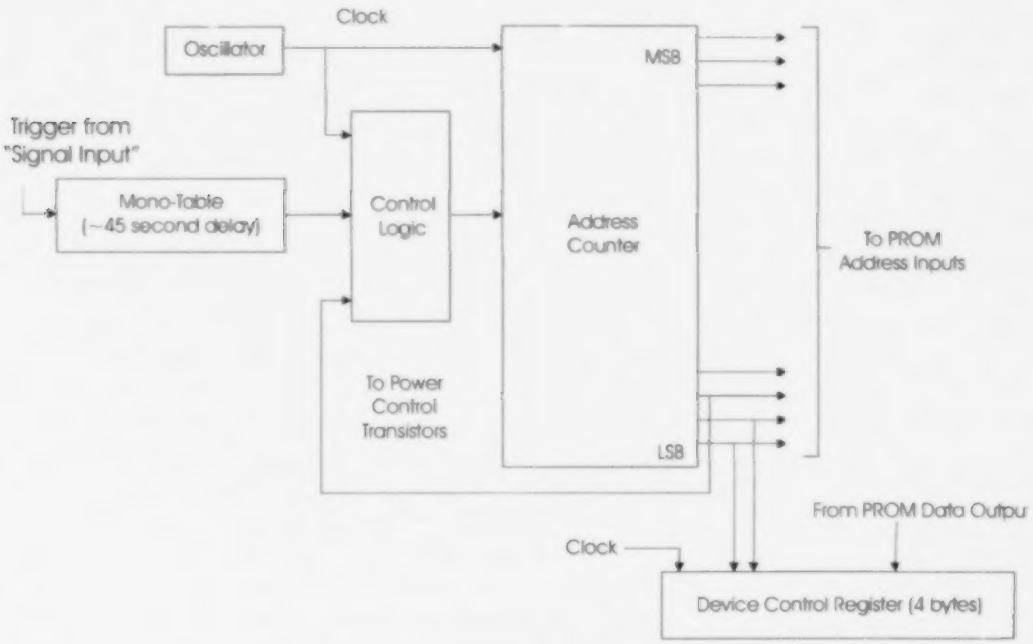

Figure 12. Timing and Address circuit concept

Power to the electronics board is turned on by a STRV utility, which subsequently provides RS422 pulse trains at 60 second intervals to trigger the operation of the electronics board. On power-up, the PROM address counter is reset to zero and power to all but the essential timing circuitry is disabled. Each trigger pulse enables a time delay of about 45 seconds. After this delay period, power is enabled to the PROM and the address counter. The first four memory locations are read out to the four-byte *"device control register"*. Each bit of these 8-bit registers is the control line of an analog switch. Subsequent trigger signals further increment the PROM address counter (in groups of 4) until the address rolls over at 2^{13}. The sequence of system states is hard-wired by the PROM implementation. The cycle repeats either by rollover of the address counter or by a power-on reset.

As soon as the new system state is latched into the device control register, power is disabled to the PROM and enabled to the analog circuit (bridge and amplifiers). The analog circuit is maintained under power until the next trigger pulse. The digitizer in the spacecraft system reads the analog level just before the RS422 lines are activated, so that this timing maximizes the analog settling time and ensures that the default mode in case of a failure is the power-on condition.

Many alternative components can be used to implement the circuit functions shown in Figs. 11-12. The detailed circuit and components were selected primarily for the timely availability of space qualified, radiation tolerant components, constrained by circuit mass, size and power specifications.

3.3 Implementation of the Electronics Board

In the final circuit, some resistors were removed from arms A, B and C in order to keep the total number of electronic switches at 40. This constraint facilitated the layout of the printed circuit board while still providing excellent bridge performance. Resistor values shown are the ones used for performance modeling and may differ slightly from the flight-unit values.

Figure 13 illustrates some details of the electronic switch implementation. The outputs of the two arms of the bridge were brought to the inputs of a differential amplifier. In fact, two separate differential amplifiers were used in parallel, in order to allow a high-sensitivity mode while still allowing for a wide range of bridge-mismatch voltages.

The flight unit used space-qualified integrated circuit switch packages in which the level translators and transistors were combined. The total number of bridge resistances was selected during implementation to allow the circuit to fit within the 100 mm x 110 mm dimensions specified by the spacecraft interface. Two electronic switches were used for amplifier gain control, allowing four positions of gain. The gains of both amplifiers were controlled by the same switches, but the gain values for a given switch setting were different for the two amplifiers, in order to achieve the desired sensitivity/range tradeoff.

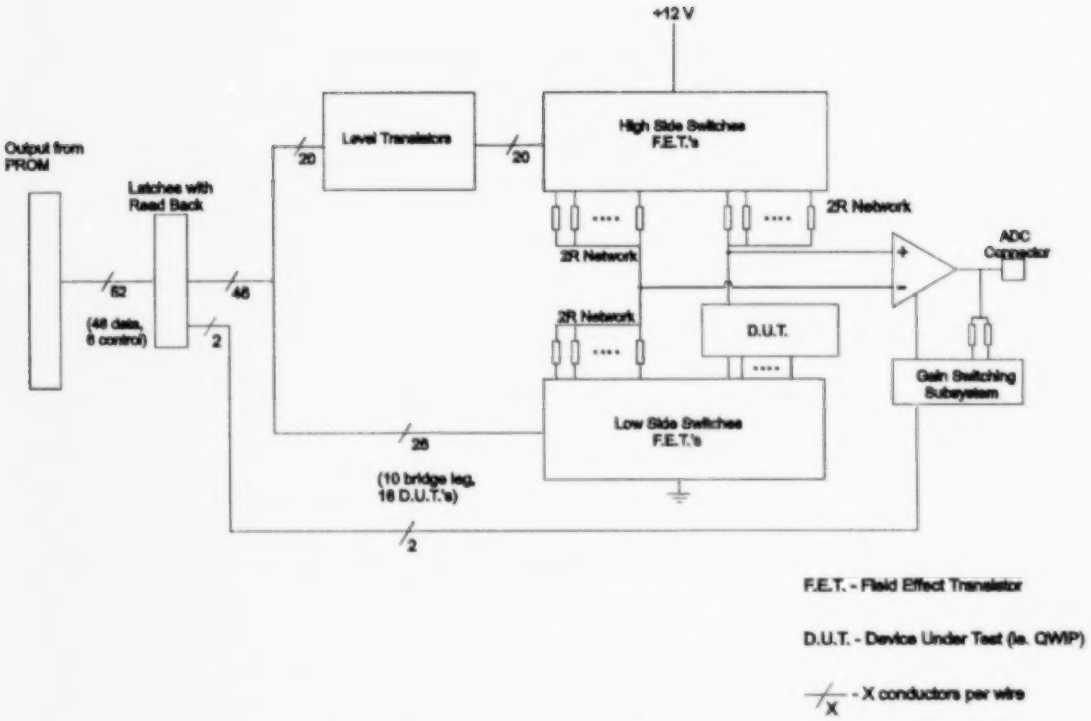

Figure 13. Implementation of electronic switching

Figure 14 shows the top surface of the multi-layer electronics pc board. The dimensions of the board are 110 mm by 110 mm. Most components are surface-mounted, and the bottom surface has a similar density of components. The board is screwed to the outer surface of the spacecraft at the corners and is protected by a passive cryocooler [7] from the direct space thermal and radiation environments. The devices under test are mounted in the cryocooler rather than directly on the electronics board and operate at a temperature that is nominally about 150 K but varies with spacecraft attitude and orbital position.

Both the analog and digital electronics use regulated 12 V DC power provided by the STRV. Suitable power control transistors allow selected circuit subsystems to be powered down to reduce average power dissipation. An RS422 differential serial link from the STRV spacecraft and its subsystems is monitored for pulse trains that trigger changes in the 'state' of the electronics board. Two (redundant) analog lines are the only outputs from the electronics board. The analog signals are digitized and stored by the STRV about once per minute, just before sending a new pulse train on the RS422 lines.

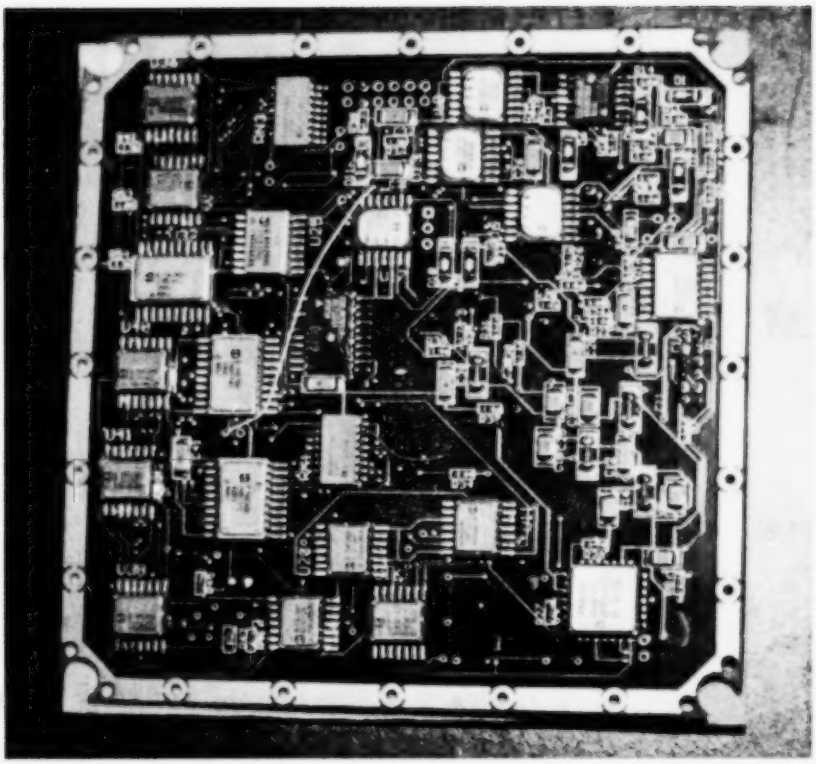

Figure 14. Photograph of flight electronic board

As described earlier, this circuit determines the resistance of a Device under Test (DUT) by comparing the voltage across the DUT to the voltage across a reference resistance in a bridge circuit. The accuracy of the measurement depends primarily on the accuracy of the reference resistances, which are hand-selected to optimize performance and have less than 0.1% change of resistance for 100 kRad total dose and no measurable change of resistance under a fluence of 10^{13} protons/cm^2 (70 MeV).

An important limitation to the operation of the Bridge circuit is the resistances of the analog switches. The switch resistance is nominally about 10^2 ohms when 'on' and 10^9 ohms or more in the 'off' state. Switch resistance varies from device to device and with temperature and time. When the device and reference resistances are greater than 10^4 ohms, this variation is generally less than 0.1%. Although the bridge resistors are very insensitive to ionizing radiation, the switch 'on' resistance does have sensitivity to ionizing radiation. To first order, this effect cancels because both arms of the bridge have similar switches. Sampling and analysis techniques further reduce the effects of switch resistance.

4. Passive Cryocooler

QWIP devices need to be cooled to temperatures low enough that thermal noise is reduced to an acceptable level. For the devices selected here, a temperature of 170 K is the upper useful operating limit. Other cryocooler requirements are listed in Table 4. Salient points in the cryocooler design and implementation are described below. Other details are provided in Mullins et al. [7].

Table 4. *Cryocooler requirements.*

requirement	notes
Test-device temperature	Below 170 K, for at least 1 hour of each 10 hour orbit.
Area of device under test	1 cm^2 on the inner (coldest) radiator
Test-device heat input	1 mW
Number of electrical wires	16
Type of electrical wires	#36 gauge manganin was used for reduced heat leakage
Mass	150 gm (cryocooler, exclusive of other system elements such as the electronics board).
Dimensions	110 x 110 x 37 mm^3
Spacecraft ambient temperature	0 – 40 deg C
Orbit	36000 km apogee, 620 km perigee, 10.5 hr period, 7 deg inclination (ie earth angular radius varies from 8.6 deg to 66 deg)
Spacecraft spin direction	Perpendicular to orbit plane, about Z axis in spacecraft coordinates
Sun illumination	Varying from – 20 deg to +20 deg off the +Z face of the satellite

Most of the specifications come from the constraints on mass, area, orbit, sun position and so forth that are placed on the spacecraft by mission or other requirements.

The cryocooler is based on principles that have been used on a number of previous designs [11], [12]. The basic concept is shown in Fig. 15.

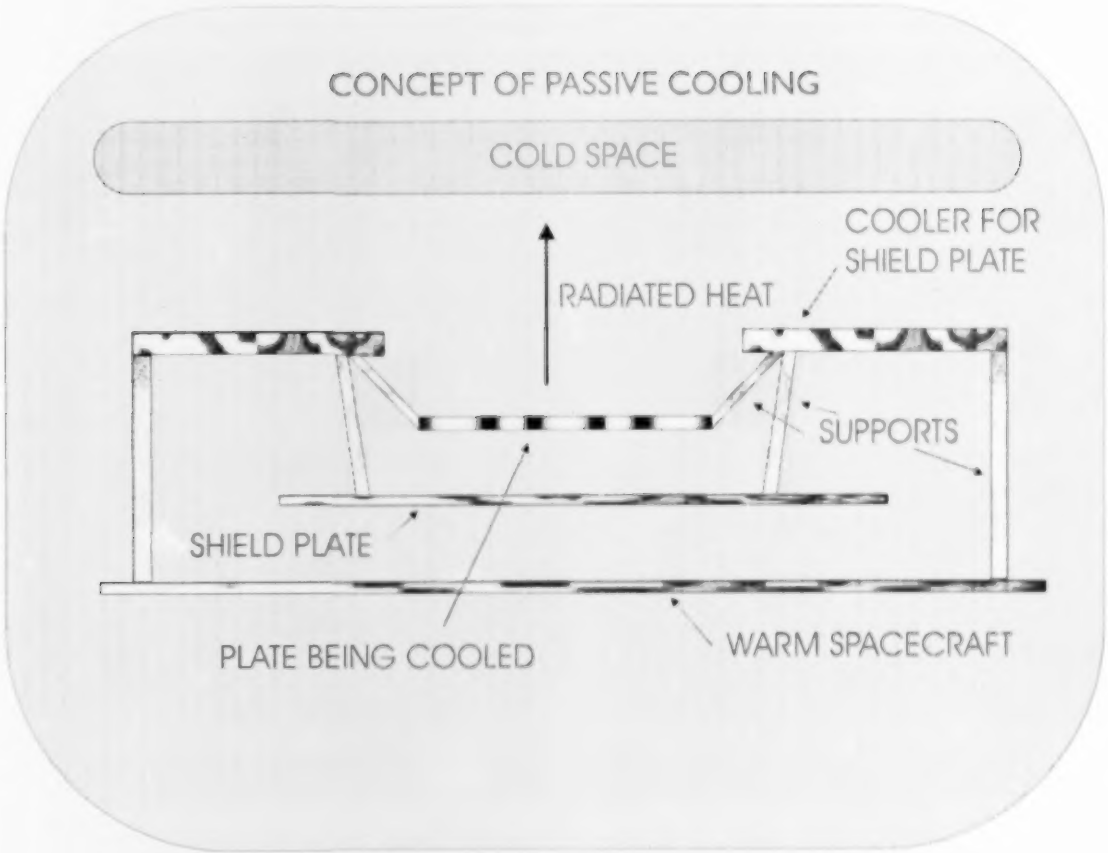

Figure 15. Passive cryocooler concept

The device under test is thermally connected to the 'plate being cooled', on the side facing cold space. In this way, the heat from the device under test is radiated into cold space without absorbing thermal radiation from warm structures of the spacecraft. A 'shield plate' isolates the 'plate being cooled' from the warm spacecraft. This shield plate is cooled by the 'cooler for shield plate'. All of the plates are rigidly mounted on supports that have low thermal conductivity and low radiant emission or absorption. The geometry of the 'cooler for shield plate' is chosen to limit the range of off-axis angles of incidence on the 'plate being cooled'.

The amount of cooling is generally proportional to the areas of the cooling surfaces. Heat loss through the supports is reduced by using long support structures. The emissivities of the various surfaces must be carefully controlled, in order to maximize radiation loss from the device under test and its cold plate, to reduce thermal radiation from hot surfaces and to reflect sunlight. Design and implementation features of the passive cryocooler are listed in Table 5.

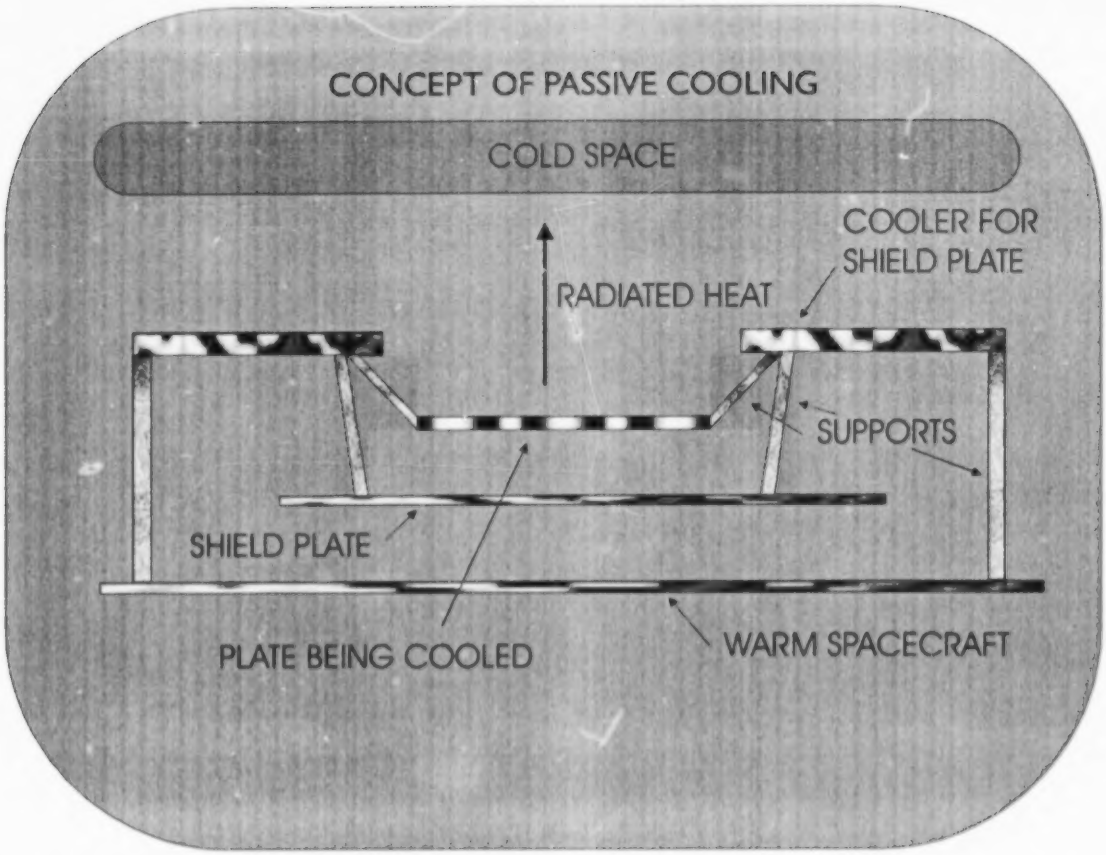

Figure 15. Passive cryocooler concept

The device under test is thermally connected to the 'plate being cooled', on the side facing cold space. In this way, the heat from the device under test is radiated into cold space without absorbing thermal radiation from warm structures of the spacecraft. A 'shield plate' isolates the 'plate being cooled' from the warm spacecraft. This shield plate is cooled by the 'cooler for shield plate'. All of the plates are rigidly mounted on supports that have low thermal conductivity and low radiant emission or absorption. The geometry of the 'cooler for shield plate' is chosen to limit the range of off-axis angles of incidence on the 'plate being cooled'.

The amount of cooling is generally proportional to the areas of the cooling surfaces. Heat loss through the supports is reduced by using long support structures. The emissivities of the various surfaces must be carefully controlled, in order to maximize radiation loss from the device under test and its cold plate, to reduce thermal radiation from hot surfaces and to reflect sunlight. Design and implementation features of the passive cryocooler are listed in Table 5.

Table 5. *Passive cryocooler features.*

Item	Comment
Mass and volume	Fitted into a small volume and has a total mass of less than 150 gm exclusive of load.
Low temperature stage	Cooling to 150K temperature is the target specification for a thermal load of 10 mW.
Angular field of view	A 60 degree field allows for attitude variations of the spacecraft while minimizing the time in orbit during which the earth is within the cryocooler field of view.
Fabrication techniques	Mechanical fabrication and coating, thermal isolators, epoxy, routing of wires and assembly and test are important fabrication factors.

Figure 16 shows in schematic form how the QWIP devices under test are mounted on the 'plate being cooled' of the passive cryocooler. Wiring of the devices used #36 manganin wire for minimum thermal conduction while still having adequate electrical conductivity.

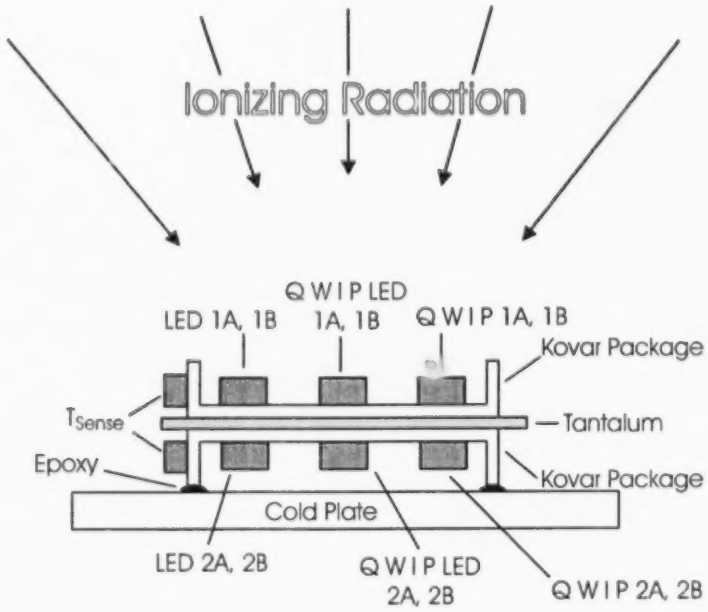

Figure 16. Placement of devices under test on cold plate

Note that there are four devices of each of three types. Each QW device on the top surface of the cold plate of the cryocooler has an identical device on the bottom surface of that plate. The latter device is partially shielded from the effects of space nuclear radiations by 1 mm of tantalum and two kovar layers. This difference in shielding allows differential measurements of the effect of radiation damage.

In the design of the cryocooler, radiative and conductive coupling among different mechanical elements is iteratively solved for selected thermal, mechanical and optical properties of the materials. Figure 17 illustrates schematically radiative coupling between different structures of the cryocooler. Each heat exchange component corresponds to the radiated power from that mechanical structure of the cryocooler and depends on area, temperature and emissivity. Except in very simple geometries, these equations are complex. Similar diagrams can indicate conductive effects. Wires and connecting rods are important factors, as is the power emitted by the device under test. Sunlight absorption can be a limiting factor in performance.

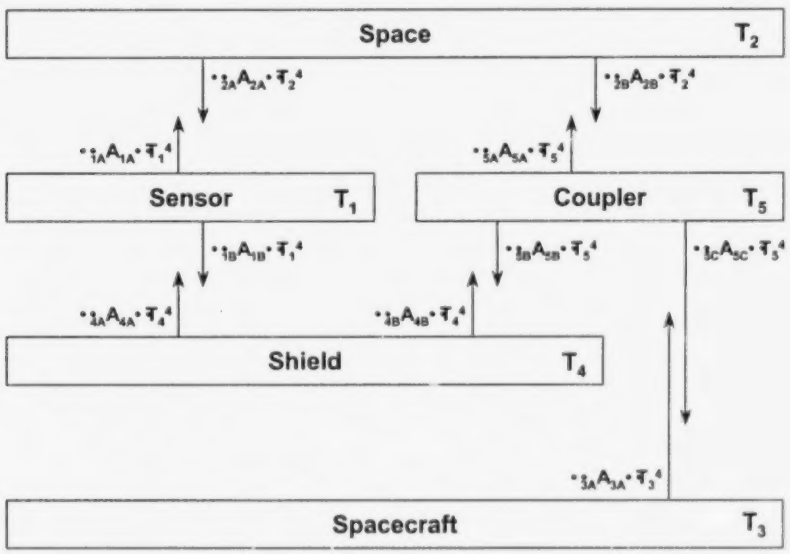

Figure 17. Schematic of radiative exchange between the payload and surroundings

When the spacecraft is close to the earth, the earth may intrude into the angular field of view seen by the cold plate, thus warming up this plate. Hence, the maximum cooling power is reduced when the spacecraft is close to the earth. The cooling power is also constrained by fabrication choices that alter the emissivity of radiating surfaces and increase the conductivity of the thermally insulating supports.

In Fig. 18, the cryocooler shield and cold plate are shown. Note that the cold surfaces are white in visible wavelengths to reflect sunlight while having a high emissivity (ie black) at thermal wavelengths. The 'cross' in the center of the cold plate retains the device carriers. Side plates prevent sunlight incidence on the cryocooler cold surfaces at large angles of incidence. Cryocooler parts facing hot surfaces are gold coated. Wires can be seen on the cold plate. These wires exit along the four insulating struts in the apertures around the edges of the cold plate.

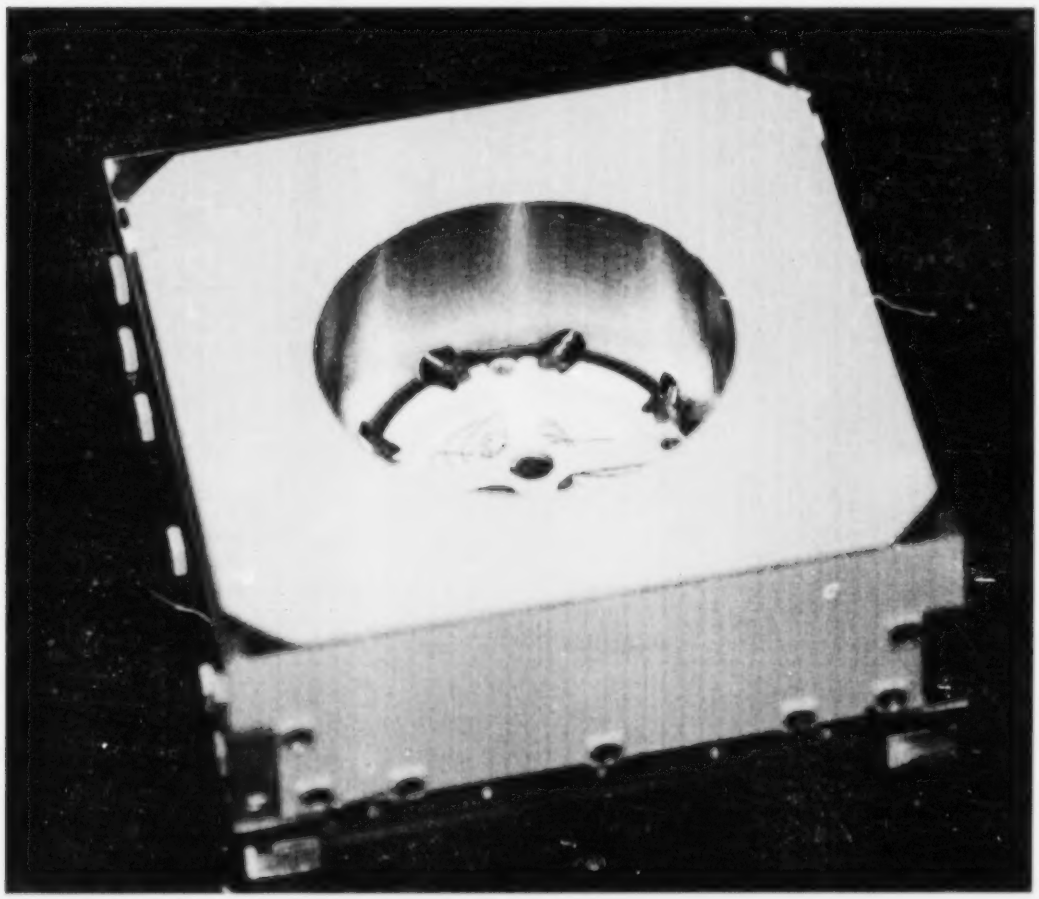

Figure 18. Top view of assembled system showing passive cryocooler

Radiant heat input from the spacecraft behind the cryocooler is limited by the shields around the outer periphery of the QWIP experiment, one of which appears in Figure 4.4, and also by a separate gold-coated aluminum radiation shield between the electronics board and the bottom of the cryocooler proper. These shielding plates are thin (1 mm) and have integral ribs for rigidity and low mass.

In Fig. 19, the attachment points of the insulating struts are shown. The nominal diameter of a strut is 0.080 inch (about 2 mm), of epoxy glass. Because of manufacturing availability, the struts have a solid cross section although annular struts would be preferred. The two square blocks with Allen screws, as well as the base plate in the figure, are not part of the cryocooler. The insulating struts are at an angle to make the conductive path longer. Each end of each strut is epoxied into a small metal block. The struts are gold-coated to reduce radiant emission.

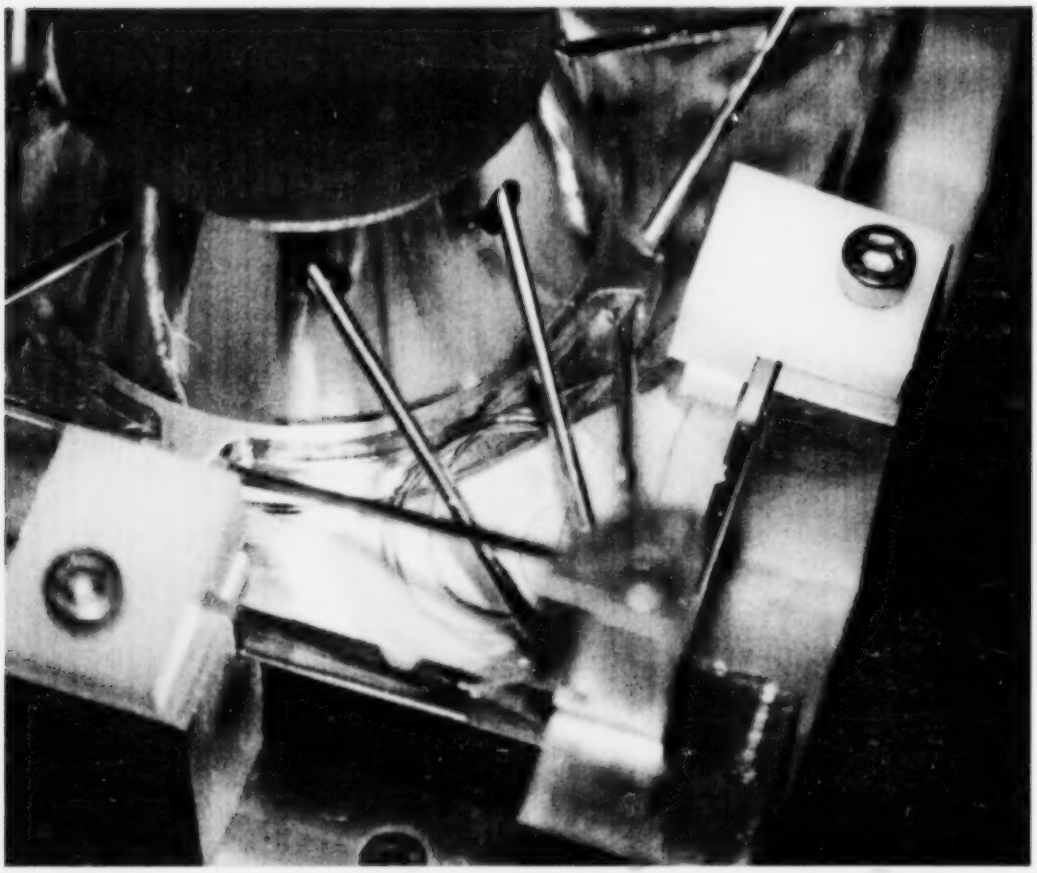

Figure 19. Insulating struts on cryocooler

Figure 19 was taken during the assembly of the flight unit, and shows some manganin wire attached to a strut while other manganin wires are coiled and have not yet been attached. The surfaces are on the spacecraft side of the cryocooler and so are gold coated to reduce emissivity. The wires contribute to radiant emission as well as conductive heat transport.

Figure 20 shows a side view of the partially-assembled QWIP experiment including the struts, the corner posts (gold plated), edge 'trim' pieces (also gold plated) and the shield between the cryocooler and the electronics board (at the top of the picture). The assembly support structure is also shown.

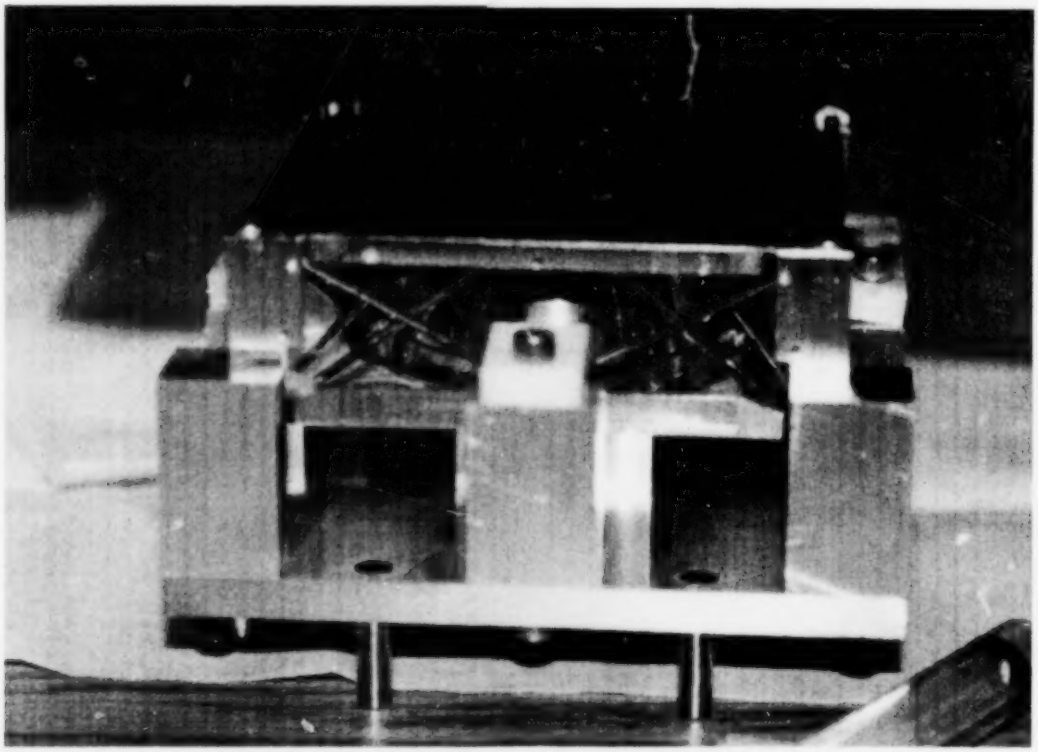

Figure 20.Side view of the cryocooler during assembly

In this figure, the cold-facing surface of the cryocooler (cf Fig. 18) is facing down and is not visible. The electronics board attaches to the top surface. Connection to the spacecraft is through clearance holes in the corner posts, and will be discussed in Section 5 of this document. The detailed wiring of the devices to their chip carriers is shown in Fig. 21. The chip carriers are 'flat packs' with wires on two sides. There are six device pairs. Each device pair is on a piece of wafer (a 'chip') about 2 mm on a side. The ground connection to each of the six chips is via conductive epoxy to the kovar chip carrier. The chips are 'wire-bonded' with gold wires to the connection pads on the edges of the chip carriers. The appropriate output wires on the chip carriers have the desired #36 manganin wires soldered to make the point-to-point connection to the electronics board. A cernox temperature sensor is attached to each chip carrier. The two chip carriers are glued (with epoxy), as shown in Fig. 21, with a 1 mm sheet of tantalum between them. Note that the top and bottom chip carriers are rotated by 90 degrees to facilitate the soldering of wires and reduce the chance of shorts between the wires from the two chip carriers.

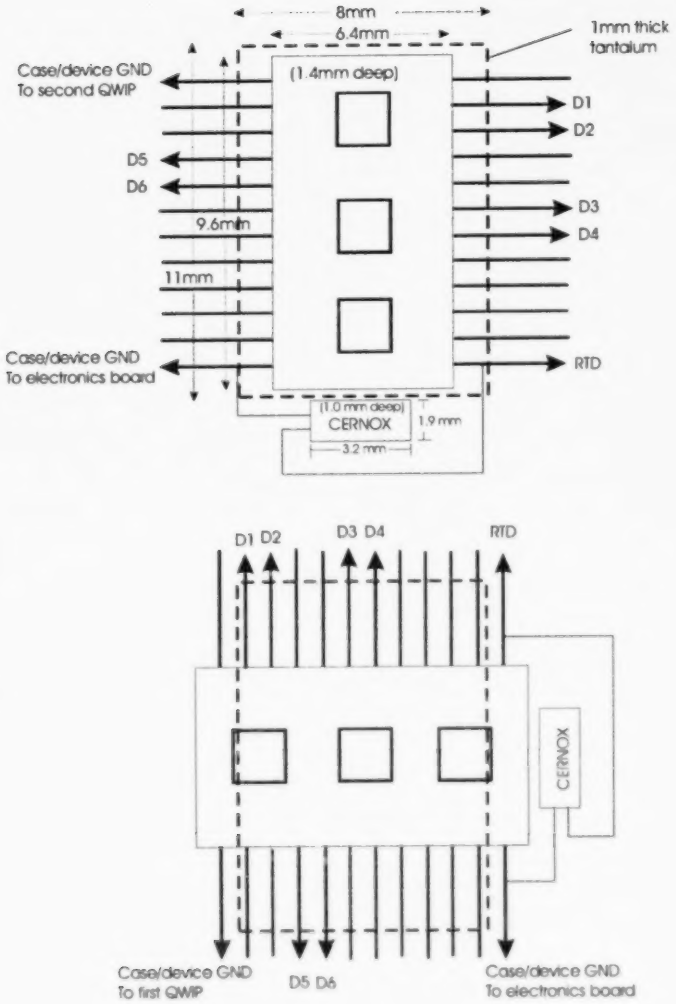

Figure 21. Wiring of the devices under test

Because the chip carriers take up significant area on the cold plate and have conductive wires, the end temperature of the cryocooler would be the details of the attachment of the DUTs. Hence, laboratory tests were performed to verify that the end temperature was in the correct range. These tests are reported in Section 7.

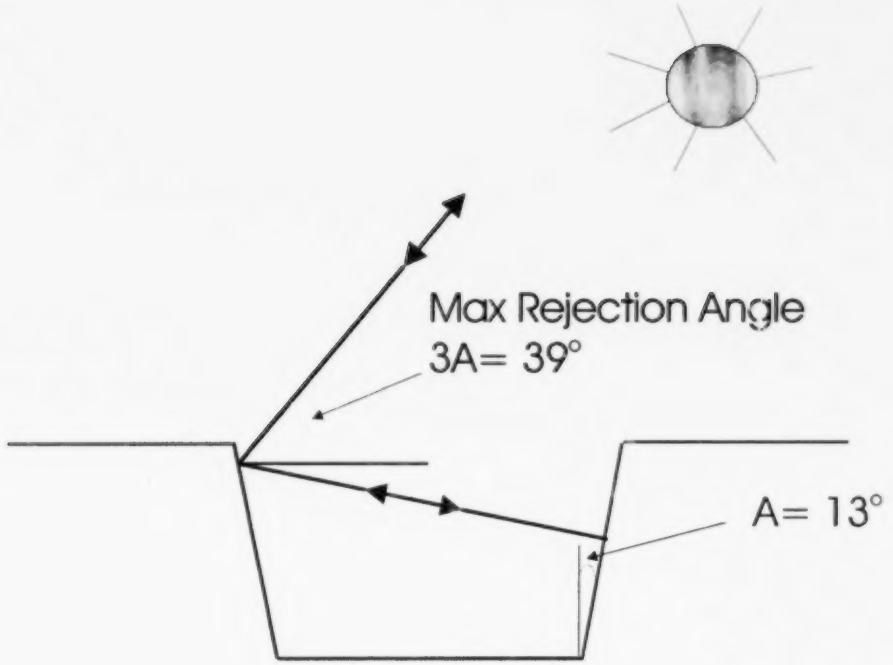

Figure 22. Rejection of sunlight by the cryocooler

Sunlight rejection is an important aspect of the design of the passive cryocooler. Sunlight absorbed on the cryocooler cold surfaces will change it from a cooler to a heater. The angular field of view of the cryocooler is determined from the placement of the cold plate with respect to the shield plate. Figure 22 illustrates this effect and the use of the shape of the shield plate of the cryocooler to reject sunlight *by reflection*. In the figure, the top surface represents the top of the shield plate while the bottom surface is the heat shield just below the cold plate and parallel to it. Ignoring diffraction and shield absorption, only light that is at larger angles (from being parallel to the shield top surface) than the 'max rejection angle' is absorbed. *The tilt angle (A=13 degrees) of the vertical part of the shield plate is carefully machined to achieve this reflection.* For sunlight rejection, the shield plate is made white at visible wavelengths while being thermally black. By contrast, the sides of the shield - from which light is reflected back into space - are gold-coated.

The attitude of the spacecraft can vary from the specified direction. For rejection of sunlight under all conditions, compensation for this variation is obtained by reducing the angular field of view of the cryocooler cold plate, which also reduces the cooling effect.

5. Interface of the CA QWIP Experiment with the STRV 1 D Spacecraft

Basically, the Canadian QWIP experiment is linked to the Electronic Test Bed (ETB), an experiment control subsystem developed by the United States Air Force on behalf of US BMDO for the STRV satellite. Mechanical, electrical and signal interfaces are described below.

5.1 Mechanical Interface

The QWIP experiment mounts on the z-surface of the STRV 1D spacecraft, as shown in Figure 1. Rather than mounting directly on the spacecraft skin, the interface is to the "Multi Function Structure" (MFS), a panel that integrates mechanical support, wiring, connectors and thermal control elements for several experiments operated by the Electronic Test Bed.

Figures 23-24 show how the QWIP experiment is installed.

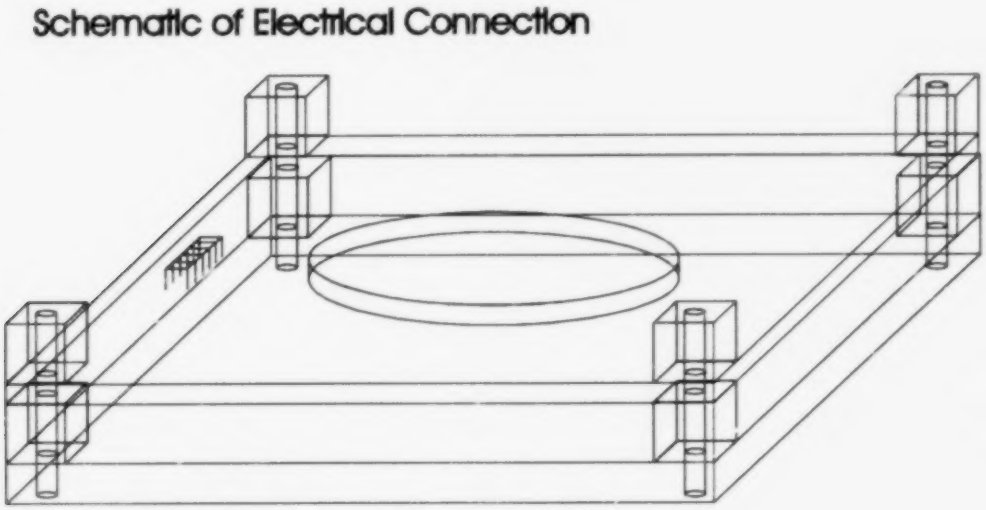

Figure 23.Schematic of electrical and mechanical connection in the CA QWIP Experiment

In Fig. 23, the electrical connector is shown on the left. It plugs into a mating receptacle in the MFS shown at bottom of sketch. The cryocooler surface at the top of the sketch faces cold space. Once the connector is in place, the QWIP experiment is screwed onto the MFS through the posts at the four corners.

Figure 24 describes the assembly of the QWIP experiment onto the MFS. Because the final connection of the flight unit is soldered, access for soldering purposes must be available. Note that test versions were generally not soldered.

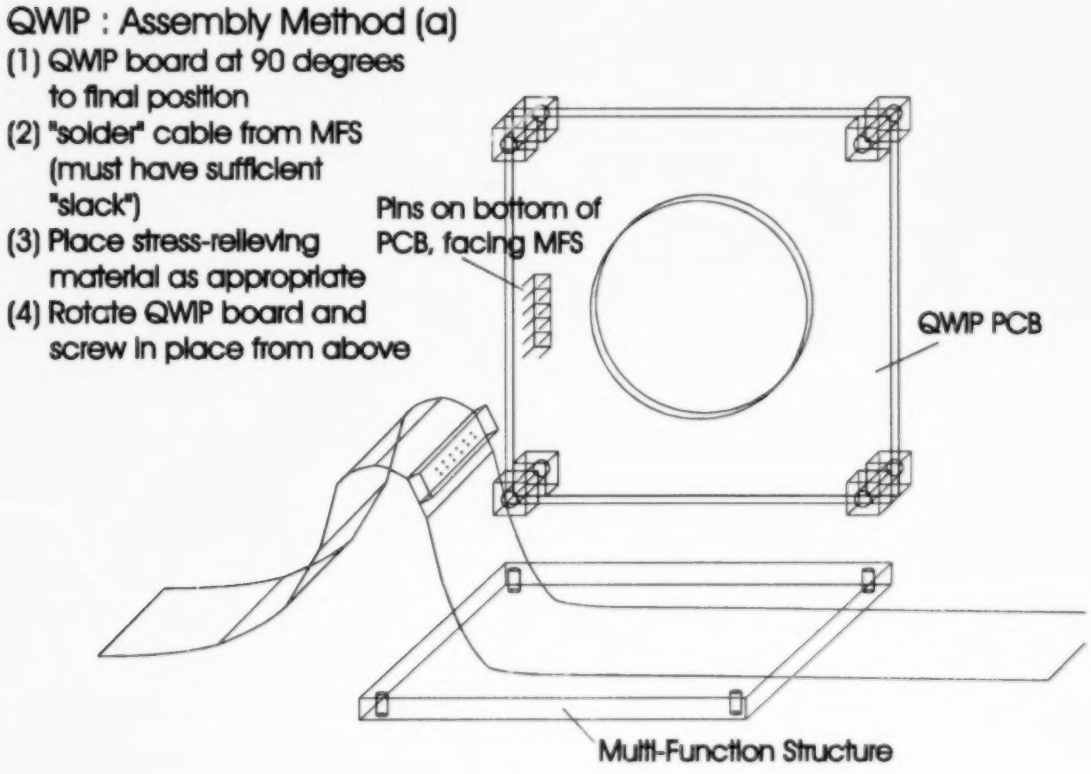
QWIP : Assembly Method (a)
(1) QWIP board at 90 degrees to final position
(2) "solder" cable from MFS (must have sufficient "slack")
(3) Place stress-relieving material as appropriate
(4) Rotate QWIP board and screw in place from above
Pins on bottom of PCB, facing MFS
QWIP PCB
Multi-Function Structure

Figure 24.Schematic of connection of the QWIP Experiment to the MFS

The thermal conductivity of the Multi-Function Structure (MFS) was tailored to ensure a uniform temperature related to the spacecraft internal temperature, which the STRV control system maintains to within defined specifications. The emissivity of the MFS was not tightly controlled but does not strongly influence the operation of the QWIP experiment or the end temperature reached by the device under test.

Note the flexible cable that is part of the MFS and is provided by the spacecraft. Without cable flexibility, soldering would not have been possible in this design. In the current design, no access from the top is available for soldering, since the cryocooler covers the top surface.

The present design allows for the entire QWIP experiment to be assembled and tested as a unit, then installed as described above. In consideration of the extended series of qualification and flight-worthiness tests, this aspect of the design was important.

5.2 Electrical and Signal Interfaces

Figure 11 identifies the electrical and signal interfaces: + 12 VDC power, an RS 422 serial link and a dual channel analog output. All of these interface connections are to the Electronic Test Bed (ETB), which in turn handles analog/digital conversion, communications with the spacecraft, triggering of events (via RS 422), power control and the storage of information before down-linking to the ground.

Power is nominally +12 VDC with modest regulation, and the electrical ground is defined with reference to the ETB rather than the spacecraft.

The serial trigger on the (differential) RS 422 line from the ETB sends a pulse train approximately every 60 seconds. This pulse train is used to control power within the QWIP experiment and to initiate a change of state, as described in Section 3. Finally, the two analog outputs of the QWIP experiment are sent to the ADC inputs of the ETB. These are digitized into 8 bits in the range between 0 and 5 VDC.

6. Data Processing

This section provides an overview of the data processing. The data processing extracts current-voltage curves from the data sequence by repeating the steps of Fig. 25 for each new data sequence. Each step uses assumptions about the supply voltage, the temperature and the state of the control switches. Any uncertainties in these assumptions are reduced if necessary by iteration of the processing steps. The iterations can be implemented on a single sequence of data or on the entire historical record of information to date.

About 20 kilobytes of data is expected per week, sufficient to measure radiation-induced shifts of resistance of 0.1% or less from week to week. With averaging, the sensitivity and accuracy will be even better. These predictions have been verified by simulated data. Systematic errors due to temperature and supply voltage drift can be reduced by modeling. In particular, the temperature profile is expected to be similar from orbit to orbit, so that the temperature correction should improve as more data is accumulated.

Note that the data processing does not require an accurate resistance model for the QWIP devices in order to determine the radiation effects or make temperature and bridge-voltage corrections.

Timing information is provided indirectly from the location of a data byte in the measurement sequence and the pre-programmed measurement times followed by the ETB instrument controller. The timing accuracy is expected to be better than 1 second, which is sufficient for the correlation of anomalies in the data with solar flares or other radiation events.

Temperature determination is a key aspect of the data analysis, since the QWIP devices are much more sensitive to temperature than to radiation fluence. Because the expected radiation effects are linear and have a slope that is very small compared to the orbital period, variations in the resistance of a QWIP device over a single orbit can be ascribed to temperature and other effects rather than to radiation. A self-consistency analysis then allows a model of temperature variation in the orbit to smooth out the random noise in the measurements and to obtain accurate values of the temperature coefficient of resistance of each device at different temperatures within the operating range. Temperature precision in the range of 0.01K has been obtained in ground-based measurements.

A new measurement is acquired approximately every 60 seconds during normal operation. Successive measurements are on different devices. The measurement sequence has been preset so that devices of the same type but with different levels of shielding are measured in succession. In the time between the measurements, the temperature is not expected to vary significantly. An accurate estimate of cumulative radiation effects can then be obtained by simply measuring the difference in the digital number obtained with the two successive measurements. This procedures scales with the effectiveness of the shielding, and is thus energy-dependent.

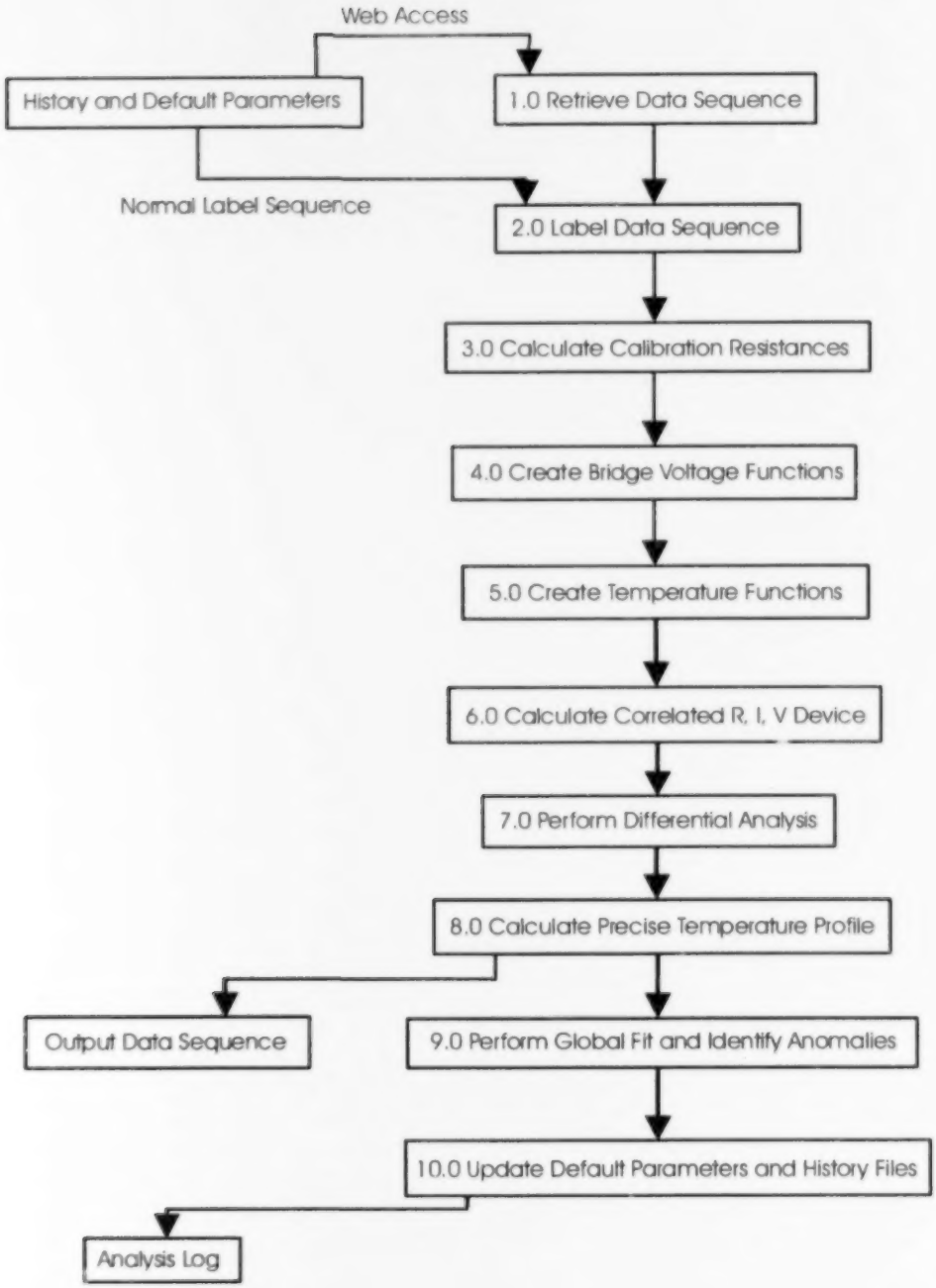
Web Access
History and Default Parameters
1.0 Retrieve Data Sequence
Normal Label Sequence
2.0 Label Data Sequence
3.0 Calculate Calibration Resistances
4.0 Create Bridge Voltage Functions
5.0 Create Temperature Functions
6.0 Calculate Correlated R, I, V Device
7.0 Perform Differential Analysis
8.0 Calculate Precise Temperature Profile
Output Data Sequence
9.0 Perform Global Fit and Identify Anomalies
10.0 Update Default Parameters and History Files
Analysis Log

Figure 25. Analysis data flow diagram

Highlights of the data processing are summarized in Table 6. Firstly, the processing is implemented in a set of spreadsheets. The use of spreadsheets allows the processing to be readily modified to adapt to unexpected situations. The systematic and random errors in the measurements are evaluated from the data sequences themselves. The analysis process can be repeated with different 'analysis constants' to iteratively refine the results. This is particularly important in view of the sensitivity of the results to the device temperature.

Table 6. *Data processing highlights.*

Item	Notes
Stepwise implementation using spreadsheets	Convenient and straightforward implementation using common commercial software tools.
Self-calibrating	Both systematic and random errors can be evaluated from the data sequences. Various analysis constants can be iteratively made more accurate.
Determination of temperature in a self-consistent manner	The devices under test are temperature-sensitive. The time scale for temperature variations is much shorter than the expected time scale for radiation effects.
Assumption of linear increase in fluence	The baseline analysis assumes that the radiation fluence increases linearly with time, so that a direct measurement of fluence is not needed.
Differential measurement	A differential measurement is available that is insensitive to systematic errors or non-radiation effects.
Implicit timing information	Timing information is derived from the data acquisition and storage procedures of the ETB.
Operation on current and historical data	Can improve accuracy by repeating the analysis with a larger dataset that includes previous measurements already analyzed.

Temperature varies over one orbital period of 10.5 hours. With a temperature coefficient of resistance of the QWIP devices of 5%/K or more, and an expected orbit-induced temperature variation of about 10 K, the resistance change due to temperature could be a factor of 2. By contrast, the expected variation of ionizing radiation, assuming a linear change, is expected to be much less than 0.1% over this time period and will be monotonic and linear. Hence, differential methods can be used to separate temperature effects from radiation effects.

To facilitate the use of differential methods for the reduction of systematic errors, the measurement sequence is structured so that a measurement on an 'exposed' device (on the top of the cold structure with no shielding) is immediately followed (ie 60 seconds later) by a measurement of the same type of device on the bottom of the structure. In this manner, the temperature is expected to have changed by a minimal amount between measurements. Furthermore, all of the bridge elements except the device under test are kept the same in the two cases. This allows a differential comparison of the resistances of the two devices with an expected precision of about 0.1%. As the radiation fluence increases over time, the more-shielded resistance is expected to show less variation. The scale factor for the difference in

fluence at the two locations - above and below the shielding – is the same for all three types of device, so that the changes in each type of device should be proportional.

Timing information is implicit in the data, based on the 60 second time interval between changes in the state of the QWIP experiment. This is linked to the orbital period in order to give a profile of temperature versus time and to correlate anomalies in the data with external events (from other experiments, the STRV or elsewhere.

Because all of the raw data is stored, the analysis method can be modified and the data re-analyzed at any time. In particular, the fitting of larger sets of data can be used to look for trends linked to nuclear radiation damage. If a radiation anomaly, such as solar flare, is recorded by space-weather sensors (perhaps external to the STRV spacecraft), the data can be searched for corresponding anomalies in the resistance of the quantum well devices.

7. Tests

7.1 Electronics Tests

Table 7 summarizes the performance of the state machine electronics board under a range of ground tests. Except for total ionizing dose under gamma rays, the board met or exceeded expectations. For the gamma ray testing, a logic chip on the board failed at 80 kRad. This failure was not critical because the chip in question was rated for 50 kRad and had additional chip-specific shielding located to reduce the expected total ionizing dose. The vibration and thermal vacuum tests followed the requirements for an Ariane 5 launch.

Table 7. *Summary of electronics tests.*

item	units	Measured value	Expected value	notes
Average power dissipation	mW	68	75	Duty cycle of 75% standby and 25% power-on; 60 second cycle time.
Total ionizing dose	Krad(Si)	89*	100	See Note below. ^{60}Co gamma rays were used.
Proton fluence	P^+/cm^2	10^{13}	10^{13}	Full performance was maintained at this fluence.
Vibration	-	Passed	-	Ariane V launch requirement
Thermal vacuum	-	passed	-	-40C to + 60C cycling while operating over 10 hours.
outgassing	Torr/minute	$< 10^{-7}$	10^{-7}	No measurable outgassing.

* A TTL logic gate IC failed at 80 kRad in the gamma ray tests. This chip was rated for 50 kRad (Si) radiation hardness and was shielded with 2 mm of tantalum. Because of the testing with gamma rays, the tantalum shielding was ineffective. After replacement of this part, the remainder of the circuit was verified to operate at specifications after 100 kRad of total ionizing dose.

The DREO radiation test facility was used to irradiate a fully populated pc board. This test facility uses a ^{60}Co gamma ray source. Irradiation was over the entire board at 5 krads/hour. The circuit was operated during irradiation and various outputs monitored for failures. A total dose of 100 kRad was applied.

The same test circuit that was tested for total dose was later irradiated at the TRIUMF facility with 70 MeV protons at a rate of about 10^9 protons/cm/sec to a level of 10^{13} protons/cm^2. No change in operation was noted either during or after the irradiation.

Vibration and thermal vacuum tests were performed at the David Florida Laboratory.

7.1.1 Electrical Power Consumption

Table 8 shows the variation of electrical power consumption for different modes of operation. During about 80% of the normal operating cycle, the circuit is in 'standby'. The low power dissipation during 'standby' emphasizes the importance of the power-down circuitry in meeting the design goal for power consumption.

Table 8. *Power for different board modes.*

Mode	Current (mA)	Power (mW)	Specifications (mW)	Note
Power Off	0	0	0	OK
Initial Power-On	13	64		RS 422 receiver chip
Standby	0.06	0.3	10	This mode is 80% of cycle
Control Electronics ON	19	93		Op amps not ON; PROM is ON

7.2 Cryocooler Tests

The cryocooler was evaluated in a laboratory cryogenic system over the temperature range expected in space, in order to verify that the expected cooling power was indeed realistic. Fig. 26 shows the temperature versus time for various points in the cryocooler, while Fig. 27 is a similar curve for the cold plate end temperature with a realistic electrical power dissipation of about 1 mW.

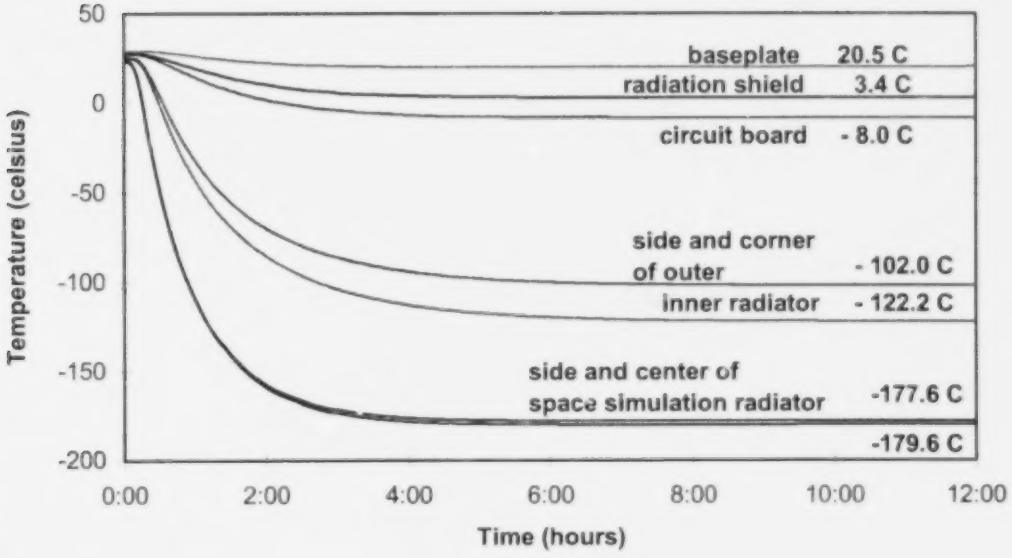

Figure 26. End temperature of cryocooler components

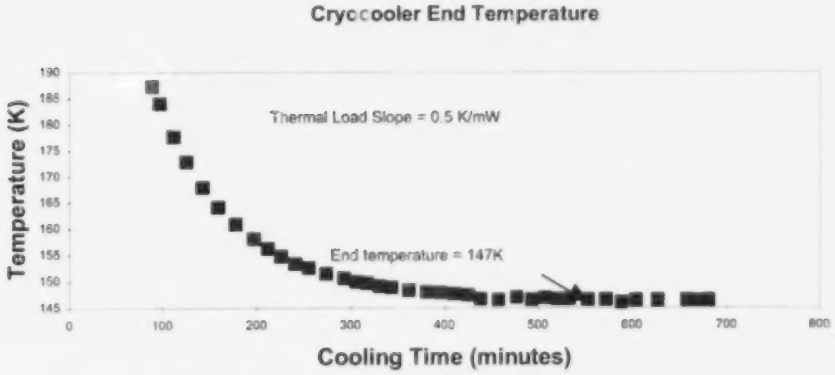

Figure 27. Cryocooler end temperature with load

7.3 Space-Based Tests

The launch of STRV 1D occurred on November 14, 2000. One sequence of test data was received from space during the 'checkout' phase of operation. This sequence contained only 15 data points, but was sufficient to indicate a temperature of about 140K at the site of the devices under test. That is, the devices were at the cold end of the expected operating range. This result verified the cryocooler design.

In addition, the test sequence verified the operation of the electronics circuitry.

No useful information was obtained on device resistance in this sequence, so that no information on radiation tolerance is available from the space experiment.

Subsequently, the STRV 1D sustained a system failure mode that has prevented further transmission of data. To date, the system has not recovered from this failure mode.

8. Conclusions

The CA QWIP experiment consisting of the quantum well IR sensors, the passive cryocooler, and the device measurement electronics was integrated on the ETB and in turn on the STRV and was launched in space successfully on board STRV 1D. The experiment performed fully soon after launch. However, a system failure on the satellite stopped all communication to all the experiments on the STRV 1C and 1D satellites. No communication has been received from any experiment on the ETB since that time.

Table 9 summarizes the status of the QWIP experiment. The QWIP electronics board is well-suited to other radiation-testing applications and can readily be implemented in a custom CMOS chip set. The cryocooler has broad applicability for space experiments. A paper on the Canadian QWIP Experiment has been presented recently at a NATO/RTO/SCI Conference [13].

Table 9. *Status summary.*

Item	Notes
Operation in space	The QWIP devices, the electronics and the cryocooler have operated successfully in space.
Radiation tolerance	At present, problems with the STRV spacecraft have prevented access to data on radiation tolerance.
Passive cryocooler instrument	A compact, modular passive cryocooler has been demonstrated in space to provide cooling to lower than 150 K for a small thermal load.
'State-machine' electronics	A PROM-based 'state machine' approach to device testing has been demonstrated in space as a subsystem connected to the Electronic Test Bed of US BMDO.
QWIP devices	QWIP devices are promising for their tolerance of the space radiation environment. Quantitative data from space is not yet available.

9. References

1. K.A. Ryden, D.G. Fearn, S.H. Alexander, "Update on Space Technology Research Vehicle", "*SPIE* Vol. 1940, p.194,1993.

2. Natural Orbital Environment Guidelines for Use in Aerospace Vehicle Development", NASA Technical Memorandum 4527, B. Jeffrey Anderson and Robert E. Smith, June 1994.

3. H.C. Liu, J. Li, Z.R. Wasilewski, and M. Buchanan, "Integrated quantum well intersubband photodetector and light emitting diode", *Electron. Lett.* Vol. 31, no.10, pp. 832-833, 1995.

4. H.C. Liu, L.B. Allard, M. Buchanan, and Z. R. Wasilewski, "Pixelless infrared imaging device", *Electron. Lett.* Vol. 33, no. 5, pp. 379-380, 1997.

5. E. Dupont, H. C. Liu, M. Buchanan, Z. R. Wasilewski, D. St-Germain, and P. Chevrette, "Pixel-less infrared imaging based on the integration of an n-type quantum-well infrared photodetector with a light-emitting diode", *Appl. Phys. Lett.*, vol. 75, no. 4, pp. 563-565, 1999.

6. H.C. Liu, J. Li, J.R. Thompson, Z.R. Wasilewski, M. Buchanan and J.G. Simmon, "Multicolor voltage-tunable quantum-well infrared photodetector", IEEE *Elect. Dev. Lett.*, Vol.14, no.12, pp. 566-568, Dec. 1993.

7. Mayes Mullins, Paul J. Thomas, John W. Harron, P. Duggan, Peter M. Sinclair, S.M. Khanna, "Passive Cryocooler for Microsatellite Payload", *SPIE* Vol 3437, "Infrared Spaceborne Remote Sensing VI", San Diego, July 1998.

8. S. M. Khanna, H. C. Liu, P. H. Wilson, L. Li, and M. Buchanan, "High energy proton and alpha radiation effects on GaAs/AlGaAs quantum well infrared photodetectors", *IEEE. Trans. Nucl. Sci.*, Vol. 43, No.6, pp.3012-18, Dec.1996.

9. S.M. Khanna, D. Estan, H.C. Liu, M. Gao, M. Buchanan, A.J. SpringThorpe, "1-15 MeV proton and alpha particle radiation effects on GaAs quantum well light emitting diodes", *IEEE Trans. Nucl. Sci.*, Vol. 47, No. 6, Dec. 2000.

10. R.A. Reed, P.W. Marchall, A.H. Johnston, J.L. Barth, C.J. Marshall, K.A. Label, M D'Ordine, H.S. Kim and M.A. Carts, "Emerging optocoupler issues with energetic particle-induced transients and permanent radiation degradation", *IEEE Trans. on Nucl. Sci.* Vol. 45 No. 6, pp 2833-2841, Dec. 1998.

11. The Infrared Handbook, William L. Wolfe, George J. Zissis, United States Office of Naval Research, 1978.

12. Satellite Thermal Control Handbook, David G. Gilmore (ed), The Aerospace Corporation Press, El Segundo, CA, 1994.

13. S.M. Khanna, D. Estan, P.J. Thomas, H.C. Liu, M. Gao, M. Buchanan and A.J. SpringThorpe "Quantum Well Infrared Photo Detectors and Light Emitting Diodes for Infrared Imaging for Space Surveillance", Proc. of NATO/RTO/SCI Symposium on "Use of Space Systems in Integrated Military Missions", held in Lisbon, Portugal May 21-23 2001.

DOCUMENT CONTROL DATA

(Security classification of title, body of abstract and indexing annotation must be entered when the overall document is classified)

1. ORIGINATOR (the name and address of the organization preparing the document. Organizations for whom the document was prepared, e.g. Establishment sponsoring a contractor's report, or tasking agency, are entered in section 8.)

Defence Research Establishment Ottawa
Ottawa, Ontario
K1A 0Z4

2. SECURITY CLASSIFICATION (overall security classification of the document, including special warning terms if applicable)

UNCLASSIFIED

3. TITLE (the complete document title as indicated on the title page. Its classification should be indicated by the appropriate abbreviation (S,C or U) in parentheses after the title.)

The Canadian QWIP Experiment on the STRV Satellite (U)

4. AUTHORS (Last name, first name, middle initial)

Khanna, Shyam M., Thomas, Paul J, Liu, H.C.

5. DATE OF PUBLICATION (month and year of publication of document)	6a. NO. OF PAGES (total containing information. Include Annexes, Appendices, etc.)	6b. NO. OF REFS (total cited in document)
December 2001	42	13

7. DESCRIPTIVE NOTES (the category of the document, e.g. technical report, technical note or memorandum. If appropriate, enter the type of report, e.g. interim, progress, summary, annual or final. Give the inclusive dates when a specific reporting period is covered.)

DREO TECHNICAL REPORT

8. SPONSORING ACTIVITY (the name of the department project office or laboratory sponsoring the research and development. Include the address.)

Space Systems and Technology Section
Defence Research Establishment Ottawa,
Ottawa, Ontario, K1A 0Z4

9a. PROJECT OR GRANT NO. (if appropriate, the applicable research and development project or grant number under which the document was written. Please specify whether project or grant)	9b. CONTRACT NO. (if appropriate, the applicable number under which the document was written)
15EP11	

10a. ORIGINATOR'S DOCUMENT NUMBER (the official document number by which the document is identified by the originating activity. This number must be unique to this document.)	10b. OTHER DOCUMENT NOS. (Any other numbers which may be assigned this document either by the originator or by the sponsor)
DREO Report TR 2001-152	

11. DOCUMENT AVAILABILITY (any limitations on further dissemination of the document, other than those imposed by security classification)

(x) Unlimited distribution
( ) Distribution limited to defence departments and defence contractors; further distribution only as approved
( ) Distribution limited to defence departments and Canadian defence contractors; further distribution only as approved
( ) Distribution limited to government departments and agencies; further distribution only as approved
( ) Distribution limited to defence departments; further distribution only as approved
( ) Other (please specify):

12. DOCUMENT ANNOUNCEMENT (any limitation to the bibliographic announcement of this document. This will normally correspond to the Document Availability (11). However, where further distribution (beyond the audience specified in 11) is possible, a wider announcement audience may be selected.)

Unlimited Announcement

13. ABSTRACT (a brief and factual summary of the document. It may also appear elsewhere in the body of the document itself. It is highly desirable that the abstract of classified documents be unclassified. Each paragraph of the abstract shall begin with an indication of the security classification of the information in the paragraph (unless the document itself is unclassified) represented as (S), (C), or (U). It is not necessary to include here abstracts in both official languages unless the text is bilingual).

This report describes the concept, design and implementation of the Canadian Quantum Well Infrared Photodetector (CA QWIP) experiment on UK STRV 1D satellite. The objective of the experiment was to check the performance and verify the effect of nuclear radiation in the space environment on Quantum Well Infrared Photodetctors (QWIP), Quantum Well Light Emitting Diode (QW LED) and QWIP/LED integrated devices designed and fabricated at the National Research Council (NRC) of Canada. The experiment was launched successfully on the STRV 1D satellite in November 2000. The CA QWIP experiment operated well in space initially soon after launch. Since then, the satellite itself has suffered a system failure that is not related to the CA QWIP experiment. This failure has prevented any communication from all experiments on the STRV 1C and 1D satellites from various countries including UK, Canada and the US.

14. KEYWORDS, DESCRIPTORS or IDENTIFIERS (technically meaningful terms or short phrases that characterize a document and could be helpful in cataloguing the document. They should be selected so that no security classification is required. Identifiers such as equipment model designation, trade name, military project code name, geographic location may also be included. If possible keywords should be selected from a published thesaurus. e.g. Thesaurus of Engineering and Scientific Terms (TEST) and that thesaurus-identified. If it is not possible to select indexing terms which are Unclassified, the classification of each should be indicated as with the title.)

Quantum well infrared photodetector, Light emitting diode, STRV, Radiation effects, Nuclear radiation, GaAs, Electron, Proton, Radiation damage, Radiation Defects, IR Imaging, Space Surveillance

Defence R&D Canada
is the national authority for providing
Science and Technology (S&T) leadership
in the advancement and maintenance
of Canada's defence capabilities.

R et D pour la défense Canada
est responsable, au niveau national, pour
les sciences et la technologie (S et T)
au service de l'avancement et du maintien des
capacités de défense du Canada.

www.drdc-rddc.dnd.ca